Treball de Fi de Grau

Grau en Enginyeria en Tecnologies Industrials

Modelling and analysis of the hydrogen flow in a PEM feeding channel

MEMÒRIA

Autor: Marina Flamarique Canellas
Director: Ramon Costa Castelló

Convocatòria: Gener 2018

Escola Tècnica Superior
d'Enginyeria Industrial de Barcelona

ABSTRACT

This project describes the modelling and the following simulations of the hydrogen feeding channel of a PEM fuel cell. Two processes are done, which are related: the filling of the system and the ejection of the gas that will react and generate electric energy.

First of all, a research is done to know better what are the PEM fuel cells in order to understand better the purpose of the project. Afterwards, the modelling of the channel is done from the continuity and Navier-Stokes equations. They are discretized setting the border conditions and the initial conditions. The next step was to simulate the filling process and the ejection of gas and the results are analyzed.

Also, even though the nature of the project is theoretical, a budget has been calculated and its environmental impact is reported. Finally, the conclusions are made, keeping in mind the results and the development of the project.

CONTENTS

ETSEIB

LIST OF FIGURES

LIST OF TABLES

NOMENCLATURE

h_f	heat of formation
ρ	density of the fluid
t	time
$\boldsymbol{u}$	velocity vector
∇	divergence operator
u	veloxity component in the z-axis
m	mass of the fluid
V	volume of the fluid
z	position in the z-axis
P	pressure
$\boldsymbol{I}$	identity matrix
$\boldsymbol{\tau}$	deviatoric stress tensor
g	body gravity accelerations
R	ideal gas constant
T	temperature
M	molar mass
μ	dynamic viscosity
υ	cinemàtic viscosity
$\dot{m}$	mass flow
r	radius
π	pi number

1. INTRODUCTION AND OBJECTIVE

1.1. Introduction

Nowadays the main energy resources are fossil fuels, such as the oil or the natural gas. The exponential increasing demand of energy decreased the availability of these sources. Also they are harmful for the environment due to the high CO_2 emissions. In order to maintain the usage of energy and decrease the CO_2 new renewable energies must be studied and applied on the new technologies. The PEM fuel cells are run with hydrogen. The advantages of this fuel are notorious: it is easy to obtain and it does not emit CO_2 while generating electricity: it only generates water and waste heat.

Even though some machines already operate with fuel cells, there are some features that must be improved in order to increase the efficiency of the cell. The recirculation of the non-used hydrogen and the constant purges of the water excess are the best solutions to achieve that goal.

In the "Institut de Robòtica i Informàtica Industrial" (IRI) there is a station with a PEM fuel cell. After different improvements such as the refrigeration of the fuel cell itself or the flow of the hydrogen with the implementation of a venturi ejector, it is time to design a proper recirculation system including the regular purges of water.

1.2. Objective

The main objective of this project is to begin the design of the hydrogen recirculation so it can be implemented in the IRI laboratory.

The design includes the modelling of the channel and the simulations of the first stages of the recirculation process: the filling of the system with the gas and the ejection of the reactant gas to the PEM fuel cell.

Once the different stages had been run, the results will be compared and analyzed in order to agree if the design can progress or a new one must be done.

2. INTRODUCTION TO FUEL CELLS

2.1. Fuel cells

There are different ways to obtain electricity depending on the type of energy conversion. For instance, the thermoelectric conversion allows to obtain electric energy from thermal energy, the hydroelectric obtains electric energy from the gravitational potential energy and fuel cells obtain it from chemical energy.

The most usual process of electrochemical conversion from fuels includes different stages of energy conversion. For instance, the process of a coal-fired power plant:

1. Combustion of the coal converts its chemical energy into heat (thermal energy).
2. The heat is used to boil water and generate steam.
3. The thermal energy of the steam is converted into mechanical energy in the turbine.
4. The mechanical energy of the turbine is converted into electrical energy (ultimate output) by a generator.

A fuel cell turns the chemical energy from the fuel into electric energy in a single step [1].

It could seem that a fuel cell is like a battery. Both of them generate electricity from electrochemical reactions and they also have a similar structure: an electrolyte, a positive electrode and a negative electrode.

However, they are not the same. The main difference between a battery and a fuel cell is how they are supplied: the fuel cell needs a continuous supply of both the oxidant and the fuel while the battery does not need a constant supply. Another difference is the quality of being discharged. This happens in a battery when it runs out of the materials that generate the chemical reaction. A fuel cell cannot be discharged: its electrodes are not subjected to the chemical reactions.

Another difference between a fuel cell and a battery is that a fuel cell generates waste heat and water. The system is required to manage them. A battery generates some heat but in a lower rate. However, the battery does not require any special equipment to manage it.

The reactants of the fuel cells are hydrogen and oxygen. The ambient air is enough to obtain the necessary oxygen for the proper running of the fuel cell. The hydrogen can be supplied as a mixture of gases, as a hydrocarbon or in its pure form.

2.2. Brief history of fuel cells

The history of the fuel cells begins in the middle of the 19th Century, when its electrochemical reaction was discovered. Since then the process has been improved several times. Throughout the development of the fuel cells the purpose of the studies had been focused in different fields and even nowadays, several studies are being done in order to improve their efficiency. In this section only the most important achievements are going to be cited and explained, in order to understand better the evolution of the fuel cells. As a summary, the Figure 2.1 shows the general timeline.

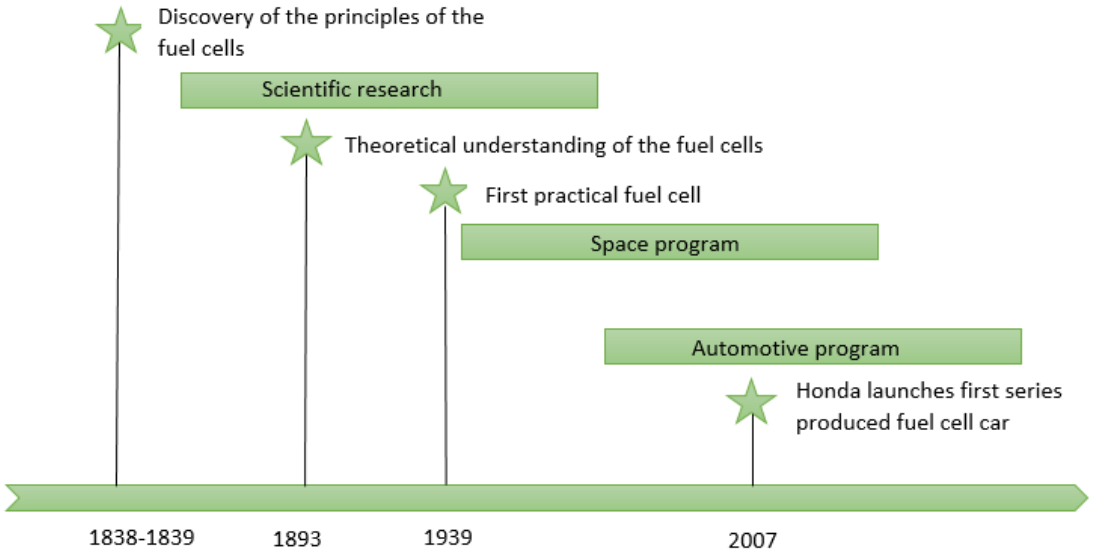

Figure 2-1 Fuel cell history timeline

In the 19th Century the decomposition of water into hydrogen and oxygen using electricity, also known as water electrolysis, was known. However, the opposite process was an unknown phenomena.

The discovery of the principles of a fuel cell can be awarded to Christian Friedrich Schönbein and to Sir William Robert Grove. Schönbein conducted the first research on a fuel cell in 1838, simultaneously Grove discovered a continuous current flowing between the electrodes. He named it gas battery and it was the first fuel cell.

After the discovery, the scientists started a research to improve and to understand the phenomena of the process. In 1893, Friedrich Wilhelm Ostwald was the first scientist to determine, experimentally, the different components of a fuel cell: the electrodes, the electrolyte, the oxidizing and reducing agents, anions and cations.

He also believed that the hydrogen would be a more common fuel in the future, when the thermodynamic engines would be replaced by fuel cells: the "Era of Electrochemical Combustion".

The next big moment of the evolution of the fuel cells occurred in 1939, when the English engineer Thomas Francis Bacon developed the first fuel cell made of hydrogen and oxygen

with practical use. During the World War II, Bacon developed a fuel cell that would run a submarine. But his most successful event was the purchase of the patent by the company Pratt and Whitney, and the use of the fuel cell in the Apollo spacecraft.

Excluding some punctual applications of the fuel cells in vans, or cars, the fuel cell was not implemented completely on the terrestrial vehicles until the nineties. For instance, the first passenger car powered by a fuel cell was launched in 1993. Since then, different car companies tried to implement this new power source.

The next highlight occurred in 2007, when Honda announced that a fuel cell-powered car would be manufactured in series: the FCX Clarity. In the 21st Century the fuel cell has been implemented in more devices besides vehicles: phones, vacuum cleaners, laptops and other electronic devices. The number of applications had increased and it is becoming the new power source [2].

2.3. Types of fuel cells

There are different types of fuel cells depending on the electrolyte they use [1]:

- Alkaline fuel cells (AFCs)
- Proton exchange membrane fuel cells (PEMFCs)
- Phosporic acid fuel cells (PAFCs)
- Molten carbonate fuel cells (MCFCs)
- Solid oxide fuel cells (SOFCs)

The different types of fuel cells have different operating temperatures and different electrochemical reactions, as it is shown in Figure 2.2.

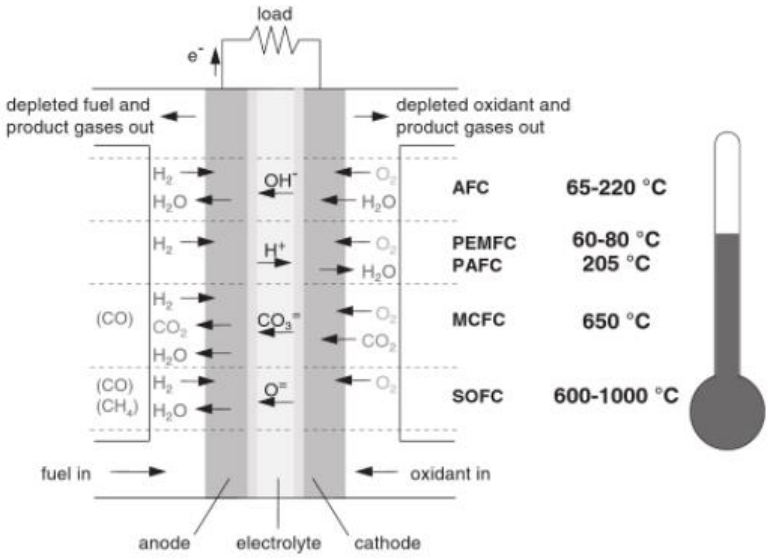

Figure 2-2 Types of fuel cells, their reactions and operating temperatures. Reproduced from [1]

3. PEM FUEL CELL

3.1. How does it work?

As it has been mentioned before, PEM stands for *proton exchange membrane* or for *polymer electrolyte membrane*. This fuel cell has a membrane with a really useful feature: it allows protons to pass through it. This membrane acts as an electrolyte and it is located between the electrodes, and there is a catalyst layer between the membrane and the electrodes.

Figure 3.1 shows a schematic diagram of a PEM fuel cell.

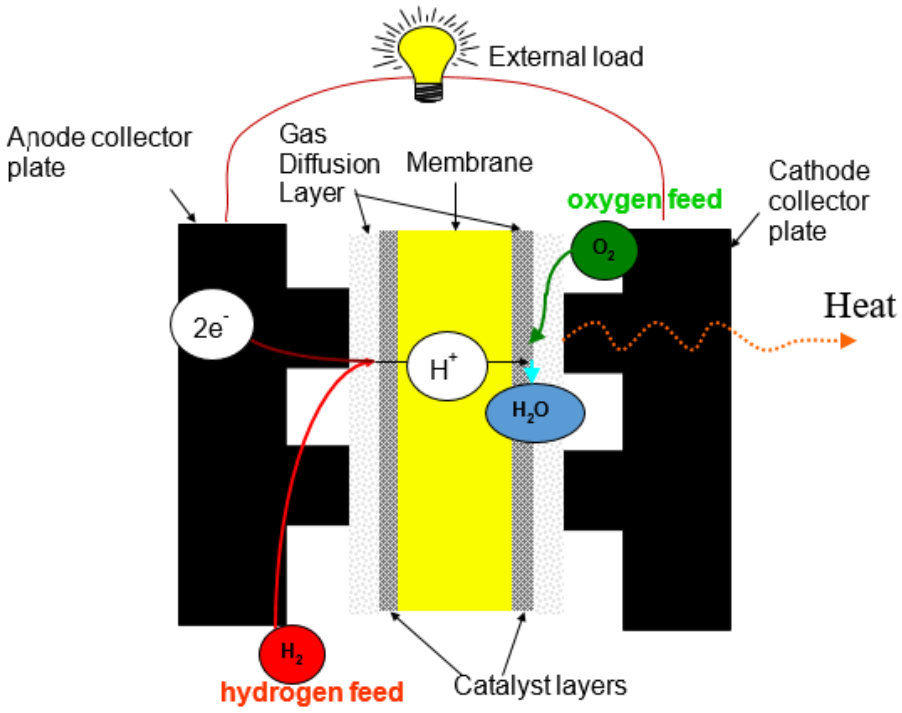

Figure 3-1 Basic principle of operation of a PEM fuel cell

A general explanation of the internal running would be the following one: the gas hydrogen is separated in protons and electrons. The protons pass through the membrane while the electrons travel through the electricity connectors until they reach the other side of the membrane. There they react with the protons and oxygen and the result is heat and water.

3.2. Basic chemistry

As it has been mentioned before, the hydrogen splits into protons and electrons:

$$H_2 \rightarrow 2H^+ + 2e^- \tag{3.1}$$

This reaction happens in one side of the membrane, the anode. In the opposite side -the cathode- the reaction is:

$$\frac{1}{2}O_2 + 2H^+ + 2e^- \rightarrow H_2O \tag{3.2}$$

Equation 3.3 shows the overall electrochemical reaction.

$$H_2 + \frac{1}{2}O_2 \rightarrow H_2O \tag{3.3}$$

3.3. Basic thermodynamics

The equation 3.3 is the reaction of hydrogen combustion. This reaction is an exothermic process, there so there is a release of heat during the process:

$$H_2 + \frac{1}{2}O_2 \rightarrow H_2O + heat \tag{3.4}$$

To calculate the heat (enthalpy) of the chemical reaction the difference between heats of formation of the products and the reactants must be calculated:

$$\Delta H = (h_f)_{H_2O} - (h_f)_{H_2} - \frac{1}{2}(h_f)_{O_2} \tag{3.5}$$

The heat of formation of elements is by definition equal to zero and the heat formation of liquid water is - 286 kJ·mol^{-1} (at 25º) [1].

$$\Delta H = (h_f)_{H_2O} - (h_f)_{H_2} - \frac{1}{2}(h_f)_{O_2} = -286\frac{kJ}{mol} - 0 - 0 = -286\frac{kJ}{mol} \tag{3.6}$$

The negative sign means that the heat from the reaction is not being absorbed, but released: it is in fact an exothermic reaction. The equation 3.3 can be rewritten as:

$$H_2 + \frac{1}{2}O_2 \rightarrow H_2O + 286\frac{kJ}{mol} \tag{3.7}$$

The equation 3.6 is just valid for an operating temperature of 25º.

3.4. Liquid water accumulation

As it has been said in the previous sections, the product of the overall chemical reaction

running in a PEM fuel cell is heat and water. It is important that these cells operate under the boiling temperature of the water at any time [3]. If they do not, the liquid could condense and block the catalyst active area and avoid the gas circulation.

Regarding the level of water, there has to be a minimum. The reason is that the membrane has to be hydrated so the proton transfer from one side to the other is correct. But an excess of water is really bad for the proper operation of the cell: it could impede the pass of the gases and there so, slow down the chemical reactions. This would decrease the cell voltage and would damage the materials.

Therefore, the PEM fuel cells need water purges, discharging the excess of water and avoiding its accumulation [4].

4. MODELLING THE HYDROGEN FEEDING CHANNEL

In the following sections, the modelling of the hydrogen feeding channel will be explained and done. And the simulations of the filling of the pipe will be run and the results will be discussed.

First of all, a coordinate system must be chosen. The geometry of the channel is cylindrical that is why all the equations will work on a cylindrical coordinate system (Figure 4.1).

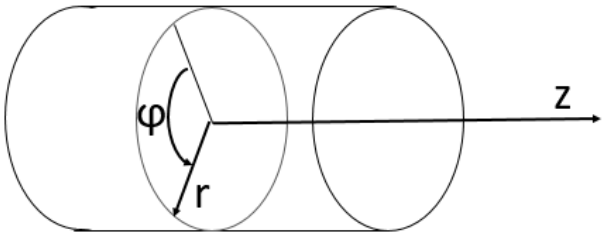

Figure 4-1 Cylindrical coordinate system

4.1. Partial equations

To observe the behaviour and the evolution of the system the study will be focused just on the dynamics of the feeding channel.

Before continuing, some simplifications must be explained. In order to simplify the calculations the fluid has been considered as a 1D flow in the z axis. That is why all the equations will suffer at least a change: transform the differential form into a 1D particular case (all the parameters will just have component on the z axis.)

4.1.1. Continuity equation

The differential form of the continuity equation is the following one [5]:

$$\frac{\partial \rho}{\partial t} + \nabla(\rho \mathbf{u}) = 0 \qquad (4.1)$$

where:

- ρ : density of the fluid [kg/m^3]
- t : time [s]
- ∇ : divergence operator
- $\boldsymbol{u}$: flow velocity vector field [m/s]

If the channel just has an entrance side and no exit, if more fluid is introduced in the system and the volume of the pipe remains constant, the density will not remain constant (4.2).

$$\rho(t) = \frac{m(t)}{V} \tag{4.2}$$

Where:

- m : mass of the fluid [kg]
- V : volume [m^3]

That is the reason why the first term of (4.1) is not null. The second term will be develop as the equation (4.3) shows.

$$\nabla(\rho\mathbf{u}) = \mathbf{u}\nabla\rho + \rho\nabla\mathbf{u} \tag{4.3}$$

The divergence operator in cylindrical coordinates is the following one [6]:

$$\nabla\mathbf{F} = \frac{1}{r}\frac{\partial(F_r)}{\partial r} + \frac{1}{r}\frac{\partial(F_\phi)}{\partial\phi} + \frac{\partial F_z}{\partial z} \tag{4.4}$$

where:

- $\boldsymbol{F}$: is a vector field

If (4.4) is applied to the velocity vector \textbf{u}, just the term belonging to the z-coordinate remains. As it has been said before, the model is 1-D in the z axial. From now on the parameter u represents the velocity in the z axial.

$$\nabla(\rho\mathbf{u}) = u\frac{\partial\rho}{\partial z} + \rho\frac{\partial u}{\partial z} \tag{4.5}$$

If the first term of the equation (4.1) is isolated, the variation of the density through the time is equal to the variation of both the density and the velocity through the position z (4.6).

$$\frac{\partial\rho}{\partial t} = -u\frac{\partial\rho}{\partial z} - \rho\frac{\partial u}{\partial z} \tag{4.6}$$

4.1.2. Navier-Stokes equation

The Navier-Stokes momentum equation can be derived as a particular form of the Cauchy

momentum equation. The conservation form of the equation of continuum motion is [7]:

$$\frac{\partial(\rho \mathbf{u})}{\partial t} + \nabla(\rho \mathbf{u} \times \mathbf{u}) = -\nabla P\mathbf{I} + \nabla\tau + \rho g \tag{4.7}$$

where:

- P : pressure [atm]
- $\boldsymbol{I}$: identity matrix
- $\boldsymbol{\tau}$: deviatoric stress tensor, which has order two [Pa]
- $\boldsymbol{g}$: represents body accelerations acting on the continuum, in this case the gravity force [m/s^2]

The simplification of the equation is the following process. First of all, the fact that the velocity has a single component decreases the vector field size and the whole equation size: the divergence operator (4.4) applies in these terms too. The second term is deleted: the vector product of the same 1D vector is 0. Also, in this specific case, the gravity force is 0. All those changes are applied in the equation (4.7) and the result is:

$$u\frac{\partial \rho}{\partial t} + \rho\frac{\partial u}{\partial t} = -\frac{\partial P}{\partial z} + \frac{\partial \tau}{\partial z} \tag{4.8}$$

The variation of the density through the time can be replaced by the equation (4.6).

$$u\frac{\partial \rho}{\partial t} = u(-u\frac{\partial \rho}{\partial z} - \rho\frac{\partial u}{\partial z}) = -u^2\frac{\partial \rho}{\partial z} - u\rho\frac{\partial u}{\partial z} \tag{4.9}$$

The pressure-related term can be modified in such a way that it only depends on the density of the fluid. That is done with the ideal gas law [8]:

$$P = \frac{\rho R T}{M} \tag{4.10}$$

Where:

- R : ideal gas constant (82,057 [atm m^3/ mol K])
- T : temperature [K]
- M : molar mass [kg/mol]

There so, the final result of the third term of the equation (4.8) is the following one:

$$-\frac{\partial P}{\partial z} = -\frac{RT\partial \rho}{M\partial z} \tag{4.11}$$

Now is time to expand the term belonging the gas friction (the last term of the equation (4.8)). For a one-dimensional fluid the equation that relates the friction with the velocity is:

$$\tau = \mu \frac{\partial u}{\partial y} \tag{4.12}$$

Where:

- τ : shear stress [Pa]
- μ : dynamic viscosity of the flow [Pa·s]

The velocity does not change through the radial axis, but there has to be a friction term in the equation so the systems conserves the energy. That is why the term is modified, and it represents the friction of the fluid due to the variation of the velocity through the z-axis.

$$\tau = \mu \frac{\partial u}{\partial z} \tag{4.13}$$

The dynamic viscosity can be substituted by the density and the cinematic viscosity:

$$\mu = \rho \nu \tag{4.14}$$

Where:

- ν : cinematic viscosity of the fluid [m^2/s]

If (4.13) and (4.14) are combined, the shear stress can be expressed as:

$$\tau = \rho \nu \frac{\partial u}{\partial z} \tag{4.15}$$

And therefore, the term is:

$$\frac{\partial \tau}{\partial z} = \frac{\partial}{\partial z}(\rho \nu \frac{\partial u}{\partial z}) = \rho \nu \frac{\partial^2 u}{\partial z^2} + \frac{\partial \rho}{\partial z} \nu \frac{\partial u}{\partial z} \tag{4.16}$$

If the equations (4.9), (4.11) and (4.16) are replaced in the initial equation (4.8), the result is:

$$-u^2 \frac{\partial \rho}{\partial z} - u\rho \frac{\partial u}{\partial z} + \rho \frac{\partial u}{\partial t} = -\frac{RT \partial \rho}{M \partial z} + \rho \nu \frac{\partial^2 u}{\partial z^2} + \frac{\partial \rho}{\partial z} \nu \frac{\partial u}{\partial z} \tag{4.17}$$

Now is time to isolate the term belonging to the variation of the velocity through the time.

That means dividing the equation by the density:

$$\frac{\partial u}{\partial t} = \frac{u^2}{\rho}\frac{\partial \rho}{\partial z} + u\frac{\partial u}{\partial z} - \frac{RT\partial \rho}{\rho M \partial z} + \nu\frac{\partial^2 u}{\partial z^2} + \frac{\partial \rho}{\partial z}\frac{\nu}{\rho}\frac{\partial u}{\partial z} \tag{4.18}$$

4.2. Discretization of the equations

To understand better how the density and the velocity of the fluid evolve during the time, a good option is to discretize the space. This means that the continuous space will be transformed into a nodes mesh, so the partial differential equations will be transformed into an algebraic equation system.

The system is 1D so the channel will be discretized only by the z-component. The space of the cylinder will be divided in nodes and the parameters' values will depend on the values of the adjacent nodes.

There so, the equations (4.18) and (4.6) will be modified. There will be three different equations for the nodes, depending where they are located. The nodes of both sides of the cylinder will be discretized by one side and fixing some values due to the bordering conditions. The central nodes of the space will have central discretizations.

In order to understand better this process, the space is divided in 3 nodes. and later it will be divided in more nodes, but the equations will remain equal. To have an idea of the spacial division, Figure 4.2 can be helpful.

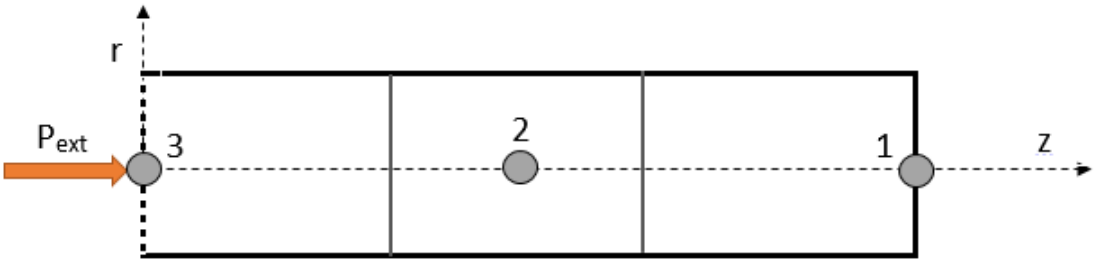

Figure 4-2 Discretization of the cylinder with 3 nodes

The node 2 belongs to the center of the cylinder and the discretization is the central type: it depends on the adjacent nodes. If this statement is applied on the differential partial equations (4.6) and (4.18) the correspondent equations are:

$$\frac{\partial \rho}{\partial t} = -u(z)\frac{\rho(z+\Delta z) - \rho(z-\Delta z)}{2\Delta z} - \rho(z)\frac{u(z+\Delta z) - u(z-\Delta z)}{2\Delta z} \tag{4.19}$$

$$\frac{\partial u}{\partial t} = \frac{u^2(z)}{\rho(z)}\frac{\rho(z+\Delta z)-\rho(z-\Delta z)}{2\Delta z} + u(z)\frac{u(z+\Delta z)-u(z-\Delta z)}{2\Delta z} - \\ -\frac{RT}{M\rho(z)}\frac{\rho(z+\Delta z)-\rho(z-\Delta z)}{2\Delta z} + \nu\frac{u(z+\Delta z)-2u(z)+u(z-\Delta z)}{(\Delta z)^2} + \\ +\frac{\nu}{\rho(z)}\frac{\rho(z+\Delta z)-\rho(z-\Delta z)}{2\Delta z}\frac{u(z+\Delta z)-u(z-\Delta z)}{2\Delta z} \tag{4.20}$$

For the most internal node (the node 1), the discretization has been done in a different way, not central but left-lateral. That means that the parameters' values of the node 1 depend on the values of the node located to the left and on the values of the node 1 itself. The equation (4.6) turns into:

$$\frac{\partial \rho}{\partial t} = -u(z)\frac{\rho(z)-\rho(z-\Delta z)}{\Delta z} - \rho(z)\frac{u(z)-u(z-\Delta z)}{\Delta z} \tag{4.21}$$

This node has a wall and that means that the particles cannot advance and they cannot get negative values because there is a positive external pressure being applied. There so the equation (4.18) for the node 1 is quite simple:

$$\frac{\partial u}{\partial t} = 0 \tag{4.22}$$

For the node 3, the discretization works similar to node 1: the parameters' values depend on the values of the node 3 itself and on the values of the node located to the right of it.

If this statement is applied on the density equation (4.16) the result is:

$$\frac{\partial \rho}{\partial t} = -u(z)\frac{\rho(z+\Delta z)-\rho(z)}{\Delta z} - \rho(z)\frac{u(z+\Delta z)-u(z)}{\Delta z} \tag{4.23}$$

As it has been done with the node 1, some border conditions must be applied with this node. The Figure 4.2 shows how this node is the first node to receive the external pressure which adds mass in the cylinder. There so, the pressure term of the node 3 depends on the values of the P_{ext}. All those changes can be seen in the following equation:

$$\frac{\partial u}{\partial t} = \frac{u^2(z)}{\rho(z)}\frac{\rho(z+\Delta z)-\rho(z)}{\Delta z} + u(z)\frac{u(z+\Delta z)-u(z)}{\Delta z} - \\ -\frac{1}{\rho(z)}\frac{\frac{RT\rho(z+\Delta z)}{M}-P_{ext}}{\Delta z} + \nu\frac{u(z+\Delta z)-2u(z)}{(\Delta z)^2} + \\ +\frac{\nu}{\rho(z)}\frac{\rho(z+\Delta z)-\rho(z)}{\Delta z}\frac{u(z+\Delta z)-u(z)}{\Delta z} \tag{4.24}$$

4.3. Equilibrium points study

The equilibrium point of an equation are those points that turn the derivative 0. If this is applied to the continuity equation (4.6) that would mean the following:

$$\frac{\partial \rho}{\partial t} = 0 = -u\frac{\partial \rho}{\partial z} - \rho\frac{\partial u}{\partial z} \tag{4.25}$$

This condition would be achieved when the variation of the density through the space is nonexistent, that is the mass distributes equally in all the pipe and the pressure is the same in all the system. Another equilibrium point is when the velocity is the same in all the system and equal to 0. There so, the equilibrium points are equal densities through all the pipe and a nonexistent velocity.

Regarding the Navier-Stokes equation (4.18), that condition means:

$$\frac{\partial u}{\partial t} = 0 = \frac{u^2}{\rho}\frac{\partial \rho}{\partial z} + u\frac{\partial u}{\partial z} - \frac{RT\partial \rho}{\rho M \partial z} + \nu\frac{\partial^2 u}{\partial z^2} + \frac{\nu}{\rho}\frac{\partial \rho}{\partial z}\frac{\partial u}{\partial z} \tag{4.26}$$

This statement would happen when the density is equal in all the cylinder and proportional to the external pressure and it would happen when the velocity is 0 in all the channel.

To check if the results of the simulation are similar to the theoretical equilibrium points, the same procedure is done with the discretized equations. The equilibrium points might be different depending on the node, due to the unlikeness of the equations. As it has been done before, to find the equilibrium points, the partial equations have to be 0.

For the central nodes this means that both the equations (4.19) and (4.20) are 0. This statement will be achieved when the densities of the bordering nodes are equal and when the velocities of the bordering nodes and the node itself are 0:

- $\rho(z + \Delta z) = \rho(z - \Delta z)$
- $u(z + \Delta z) = u(z - \Delta z) = u(z) = 0$

If the study is now focused on the most internal node, now the equations (4.21) and (4.22) must be equal to 0. The second one already accomplishes this statement. For the first one, the densities of the adjacent node and the node itself must be equal and the velocity of the adjacent node must be 0 too:

- $\rho(z) = \rho(z - \Delta z)$
- $u(z - \Delta z) = u(z) = 0$

For the most external node, the equations are (4.23) and (4.24). This last equation has the

external pressure as a boundary value. There so, the equilibrium point of the density is when the internal pressure of the node is equal to the external pressure. This statement determines the density of the node, and so the density of the adjacent node. Also, the velocities of the adjacent node and the node itself must be zero:

- $P_{ext} = \frac{RT\rho(z+\Delta z)}{M}$
- $\rho(z) = \rho(z + \Delta z)$
- $u(z) = u(z + \Delta z) = 0$

If all the different conditions are compared, the equilibrium points are the same that the theoretical ones. The system reaches the steady-state when the density of all the nodes are the same and proportional to the external pressure and also when the velocities are equal to zero.

4.4. Lineal system

In order to compare better the behaviour of the system on the equilibrium points, it has been linearized. With Matlab commands the transfer function of the system has been calculated. The input signal is the external pressure and the output signal is either the velocity or the density of one of the nodes. Once the function transfer is calculated, a graph is developed to see the response of the function in front of a unitary step sign.

This process has been done with a 3-node model and a 20-node model. For the 3-node model, the outputs signals are the velocity and the density of the node 2, while for the 20-node model, the output signals are the parameters of the node 10.

The following function transfer (4.27) belongs to the velocity of the node 2 of the 3-node model:

$$G(s) = \frac{0.61983s^2(s + 2.023e11)}{s(s^2 + 0.3712s + 5.516e08)(s^2 + 0.6205s + 1.003e11)} \tag{4.27}$$

The function transfer (4.28) belongs to the density of the node 2:

$$G(s) = \frac{45.455s(s^2 + 0.4959s + 1.003e11)}{s(s^2 + 0.3685s + 1.097e09)(s^2 + 0.6232s + 1.009e11)} \tag{4.28}$$

The Figures 4.3 and 4.4 show the time response of the transfer functions (4.27) and (4.28).

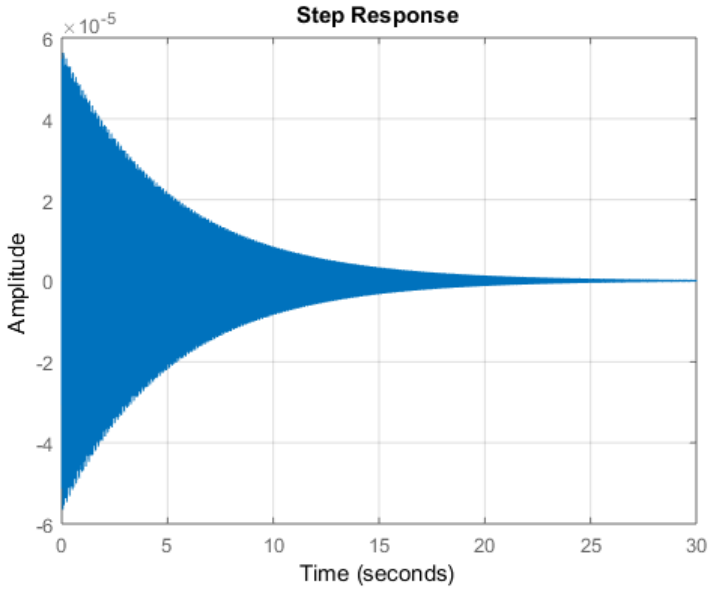

Figure 4-3 Time response of the function transfer for the velocity of the node 2

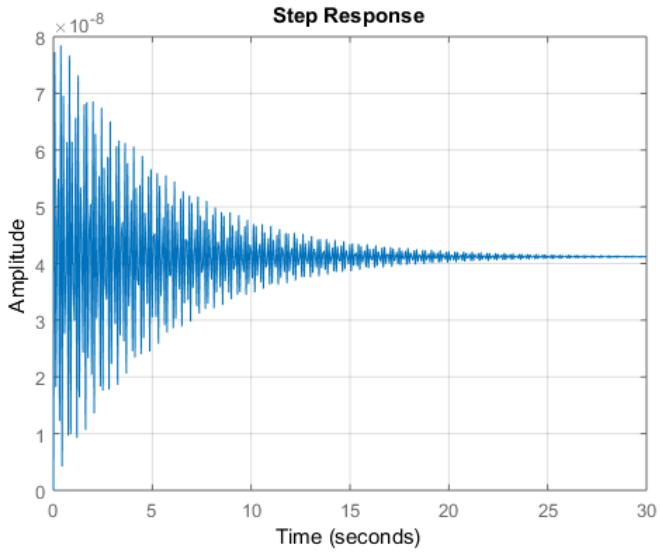

Figure 4-4 Time response of the function transfer for the density of the node 2

The responses of the node 10 (from the 20-node model) in front of a step signal are Figure 4.5 for the velocity and 4.6 for the density.

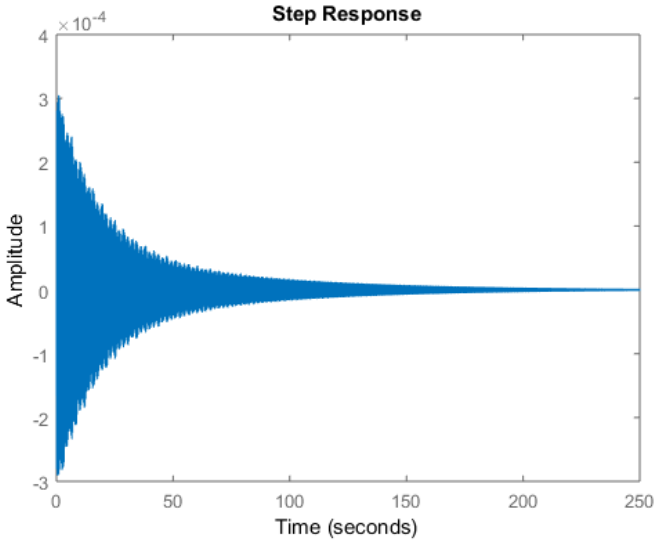

Figure 4-5 Time response of the function transfer for the velocity of the node 10

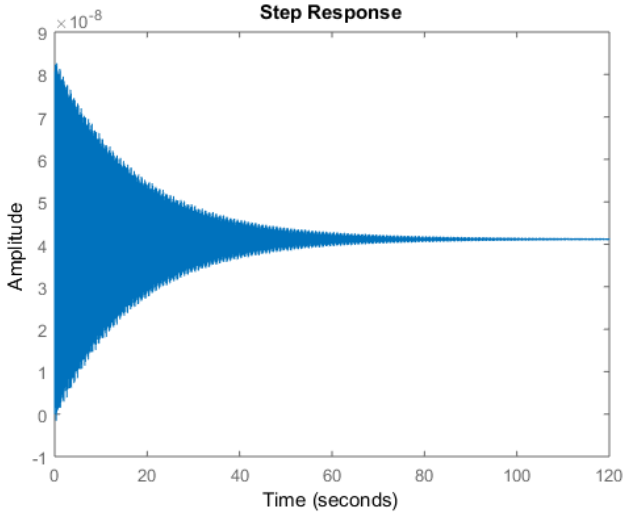

Figure 4-6 Time response of the function transfer for the density of the node 10

4.5. Simulation

The simulations had been run with the numerical computing software Matlab and its files extension Simulink.

Besides the values of the hydrogen gas and other parameters, the external pressure is an important parameter and its changes modify in a significant way the simulation results. The values of the density and speed inside the cylinder are too small compared to the pressure values. With such a numerical difference the simulation gives some mistakes and cannot be completed. So instead of applying a constant pressure it will be applied as a saturated ramp.

The entrance will start at the second 0,03 and the slope is the difference between P_{ext} (final

external pressure) and P_{ext0} (initial external pressure) divided by a 1,5 factor. The initial external pressure is not 0, because the cylinder is not empty. That is to avoid a vacuum effect. The final value has been fixed as the double of the initial one. When the ramp reaches the final value it is saturated to prevent it from increasing. The equations that show the value and the relation between the external pressure and the initial density are:

$$P_{ext}0 = \frac{RT\rho_{i,0}}{M} \tag{4.29}$$

$$P_{ext} = 2\frac{RT\rho_{i,0}}{M} \tag{4.30}$$

Where:

- P_{ext0} :initial external pressure
- P_{ext} : final external pressure
- $\rho_{i,0}$: initial density of the node in contant with the external pressure

The evolution of the external pressure can be seen in the Figure 4.7.

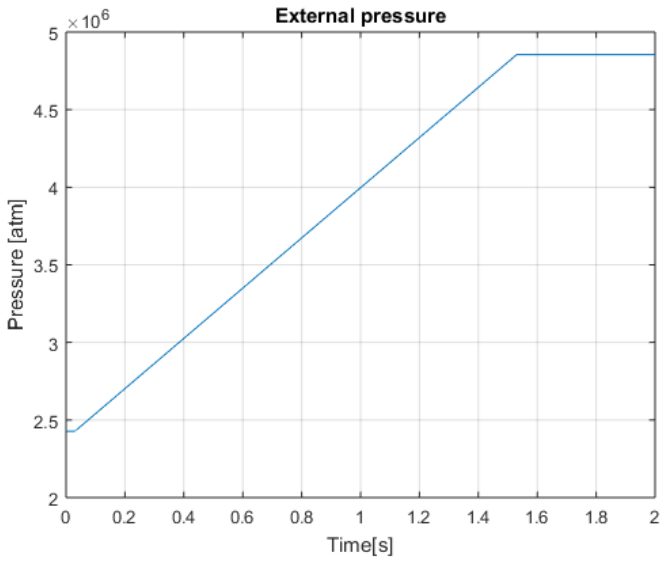

Figure 4-7 Evolution of the external pressure

To set the distance between nodes, a supposition has been made: the cylinder total length is 30 cm. So the node's size depends on the number of nodes (n). These value, the constants and others parameters had been fixed as it can be seen on the Table 4.1.

Constants	Value	Units
n	3-5-10-20	-
z	$\frac{0,3}{n}$	m
R	82,057	$\frac{m^3 atm}{mol K}$
T	298,15	K
M	0,00201588	$\frac{kg}{mol}$
ν	$3\ 10^{-5}$	m^2/s
$\rho_{i,0}$	0,2	$\frac{kg}{m^3}$

Table 4-1 Names, values and units of the parameters and the initial conditions

4.5.1. Simulation (3 nodes)

In this section the results of the simulation with 3 nodes are shown.

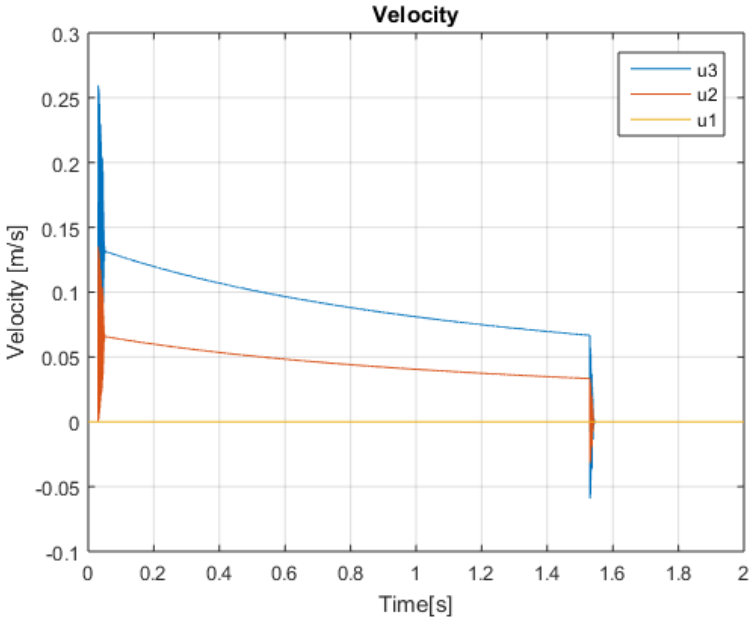

Figure 4-8 Velocities of the simulation with 3 nodes

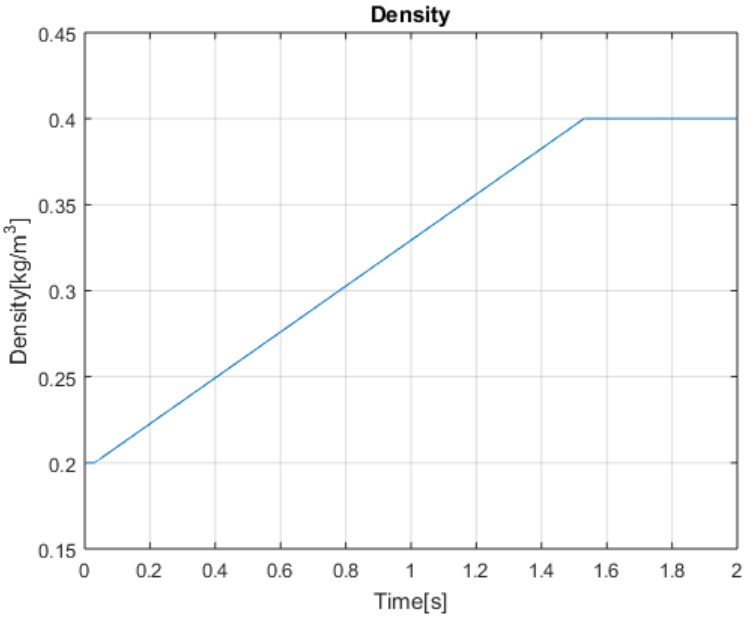

Figure 4-9 Densities of the simulation with 3 nodes

The 3-node model has been simulated with a step signal too so the comparison with the linearized system is possible.

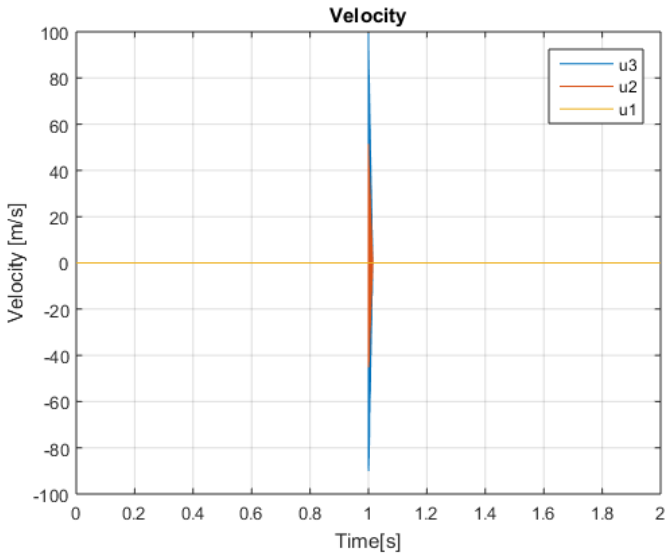

Figure 4-10 Velocities of the 3-node model with a step signal entrance

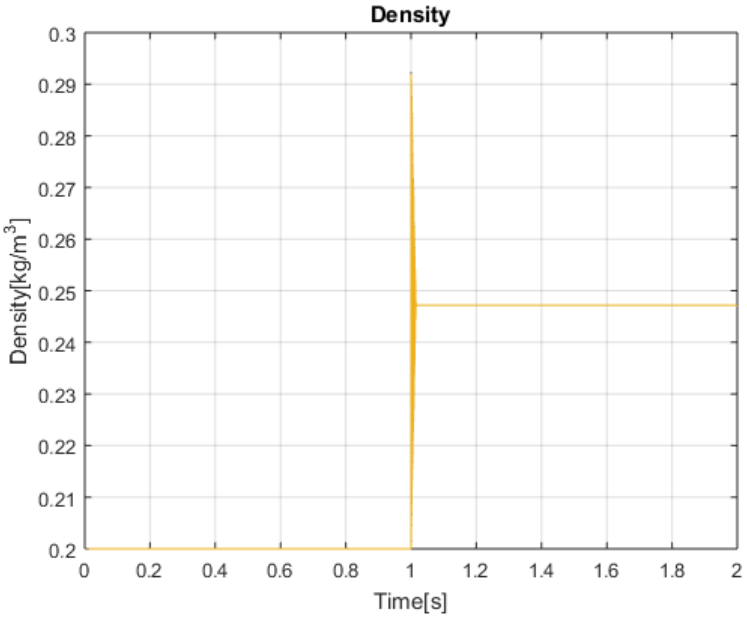

Figure 4-11 Densities of the 3-node model with a step signal entrance

4.5.2. Simulation (5 nodes)

The results of both the velocities and the densities of the model discretized with 5 nodes are the following graphs:

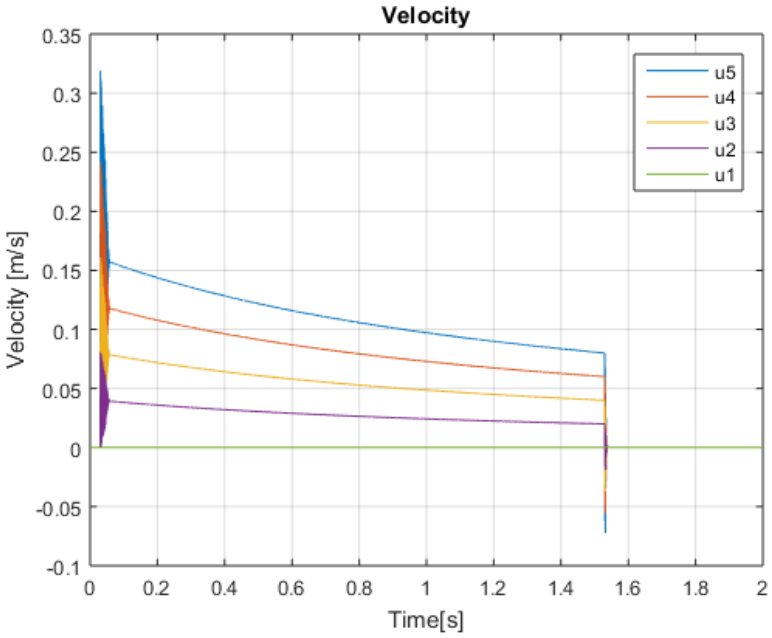

Figure 4-12 Velocities of the simulation with 5 nodes

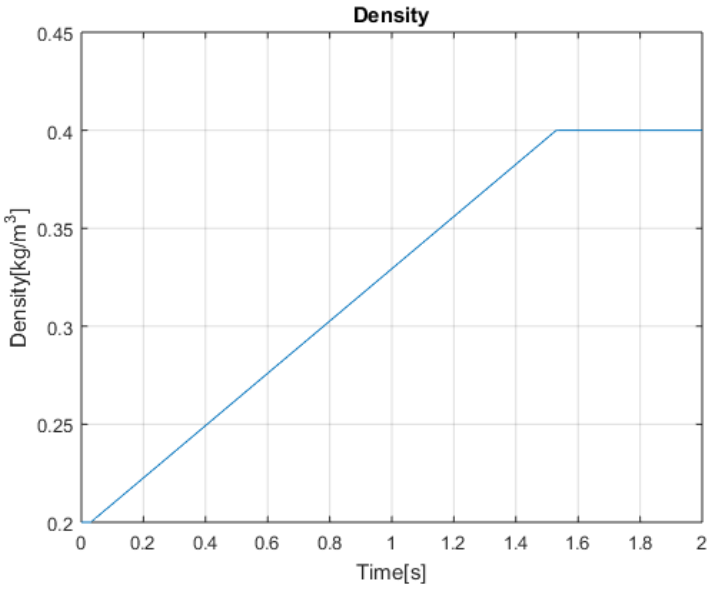

Figure 4-13 Densities of the simulation with 5 nodes

4.5.3. Simulation (10 nodes)

The results of both the velocities and the densities of the model discretized with 10 nodes are the following graphs:

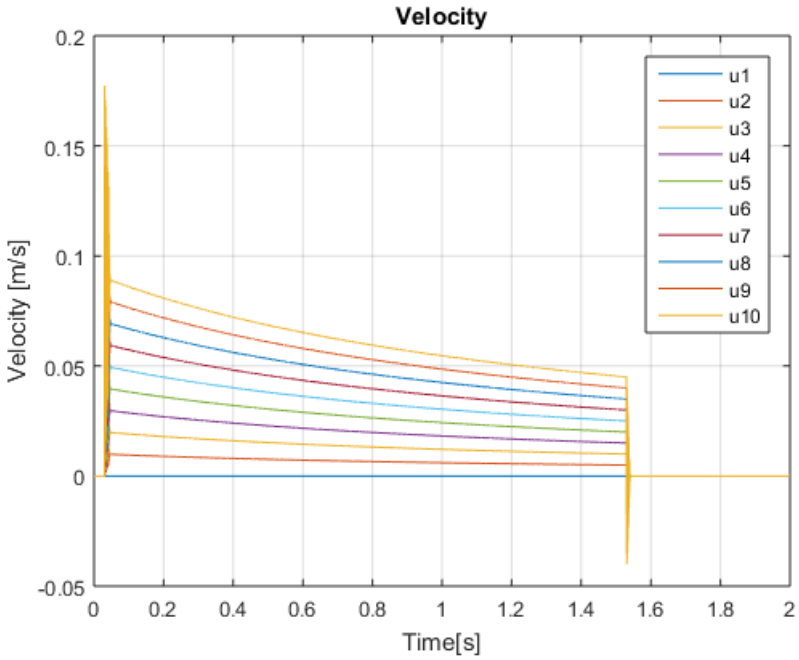

Figure 4-14 Velocities of the simulation with 10 nodes

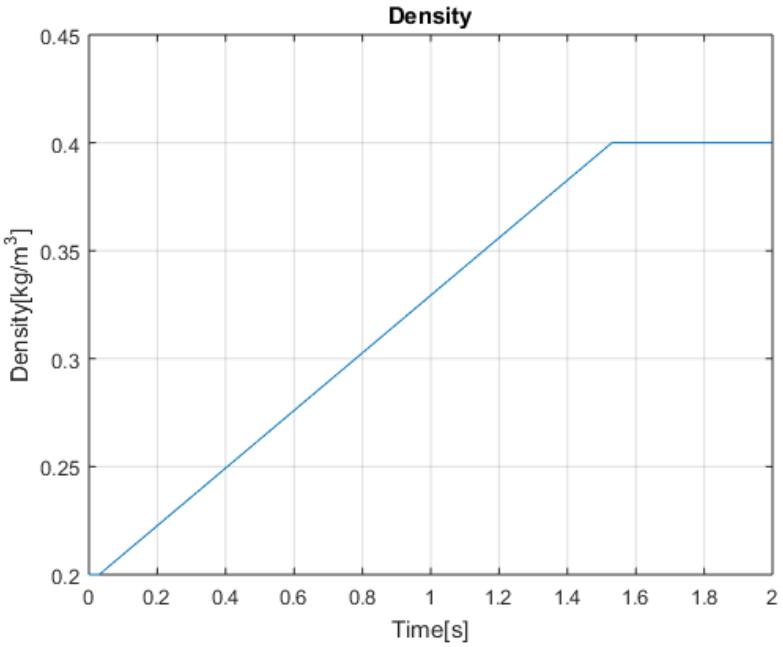

Figure 4-15 Densities of the simulation with 10 nodes

4.5.4. Simulation (20 nodes)

The results of both the velocities and the densities of the model discretized with 20 nodes are the following graphs:

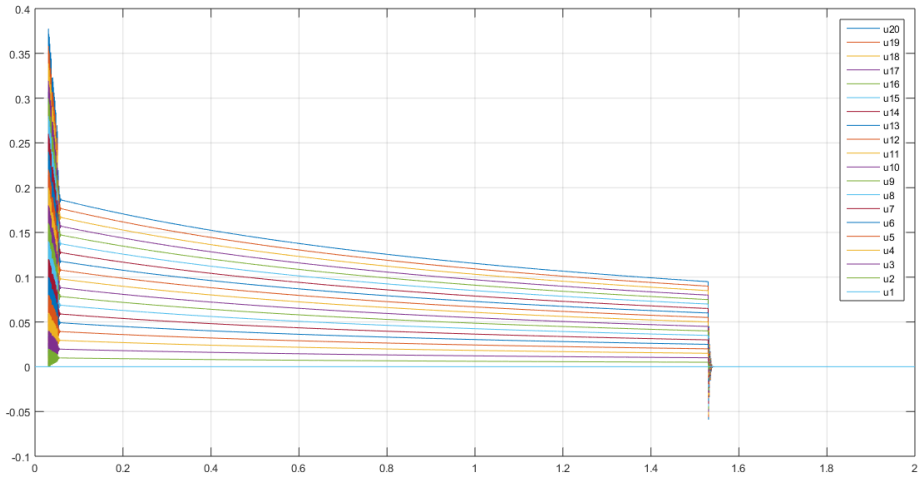

Figure 4-16 Velocities of the simulation with 20 nodes

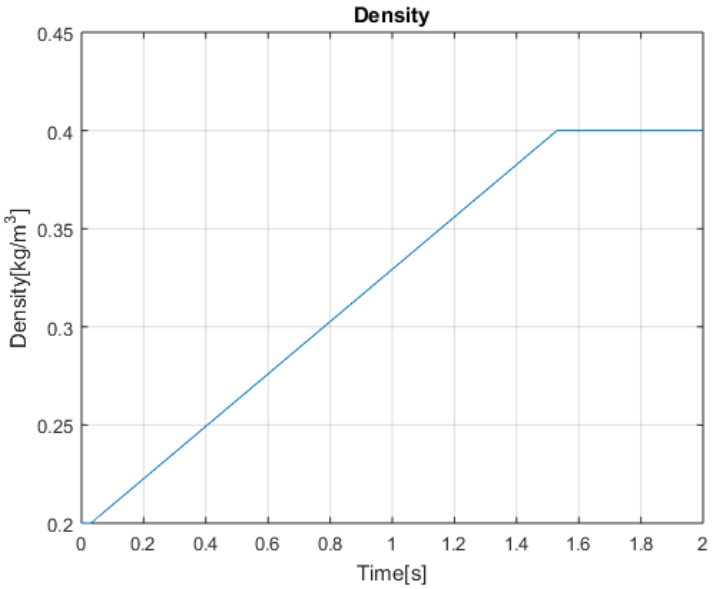

Figure 4-17 Densities of the simulation with 20 nodes

In order to compare better the response of the linearized system of the 20-node model, another simulation has been done. The response of the node 10 in front of a step signal are the following pictures (Figure 4.18 and Figure 4.19):

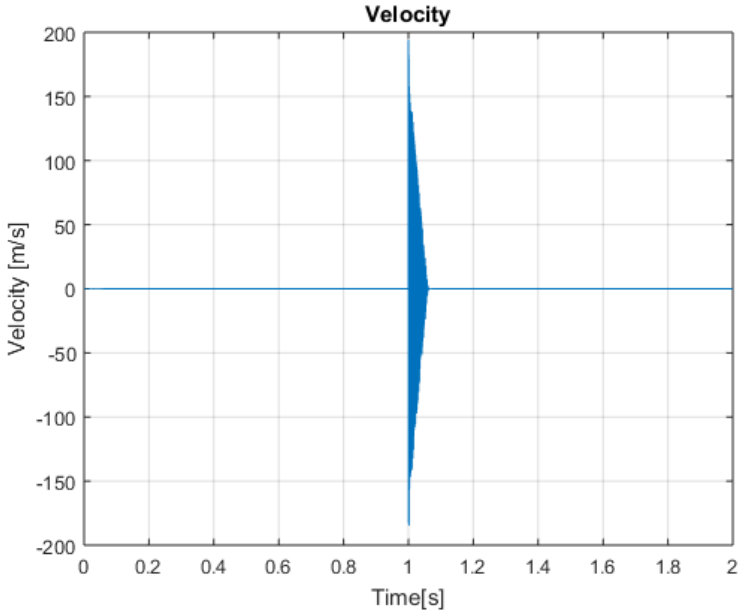

Figure 4-18 Velocity of the node 10 (20-node model) in front of a step signal

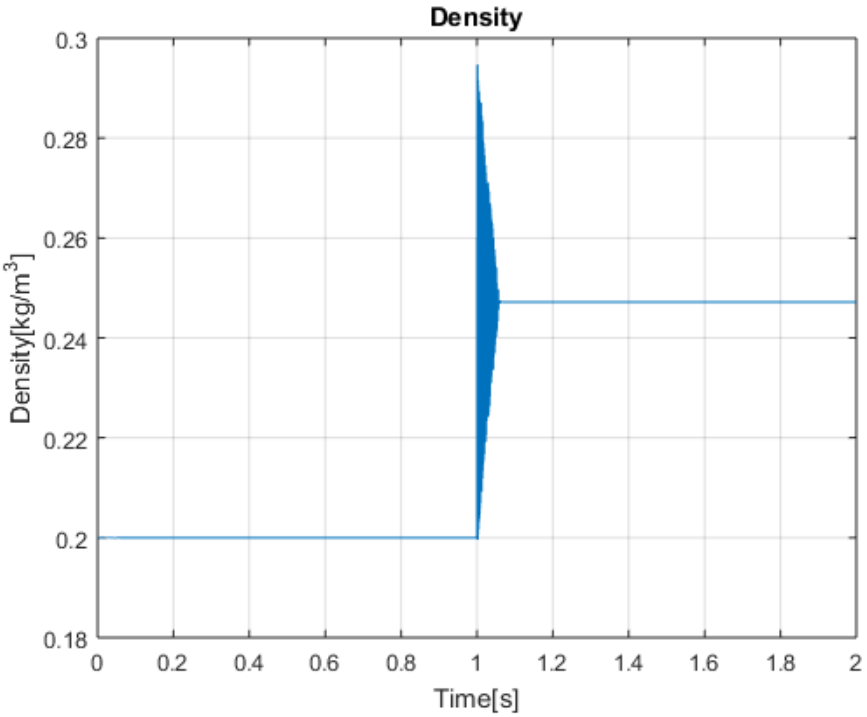

Figure 4-19 Density of the node 10 (20-node model) in front of a step signal

4.5.5. Comparison of the results

In this section the different results obtained from the previous simulations is analyzed and compared.

It is simple to observe that the system starts evolving from the second 0,03, when the external pressure starts to increase. Another common point is the moment when the system reaches the steady-state: the second 1,53. This is the same instant when the external pressure is saturated.

The density graphics are the same for all the simulations: they start at 0,2kg·m^{-3} and finish at 0,4kg·m^{-3}. The shape of the graphic is a slope that reminds of the external pressure's slope (Figure 4.7). The reason of the similarity between both graphs is the relation between the pressure and the density (4.10).

Regarding the velocity graphics, their shape is not a slope, not even a straight line. But there is something common in all the graphs: the velocities decrease gradually and then they stop to become 0. Before reaching the highest point and before becoming 0, the velocity has some oscillations. In order to compare them, the max step size has decreased from 0.001 to 0.0001, and just the most external node has been studied, in the simulation of 3 nodes (Figure 4.20) and the simulation of 20 nodes (Figure 4.21).

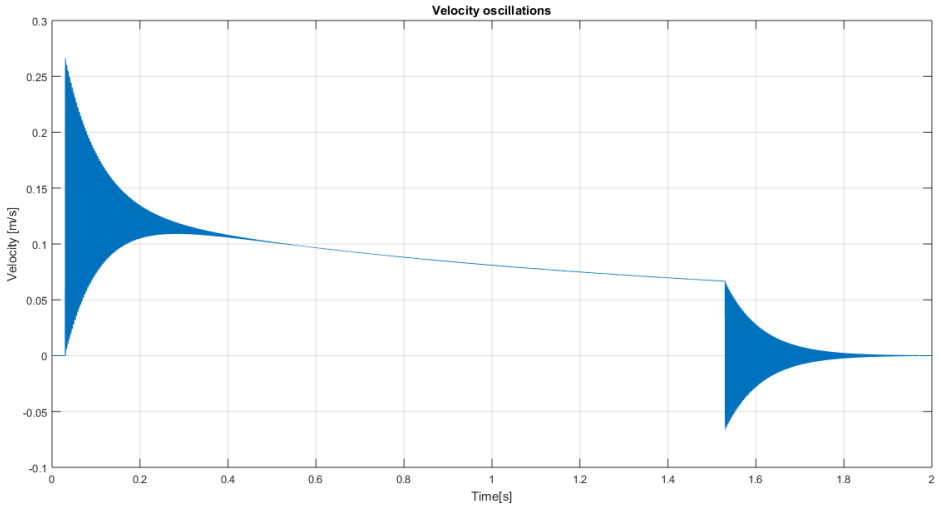

Figure 4-20 Velocity of the node 3 (Simulation of 3 nodes)

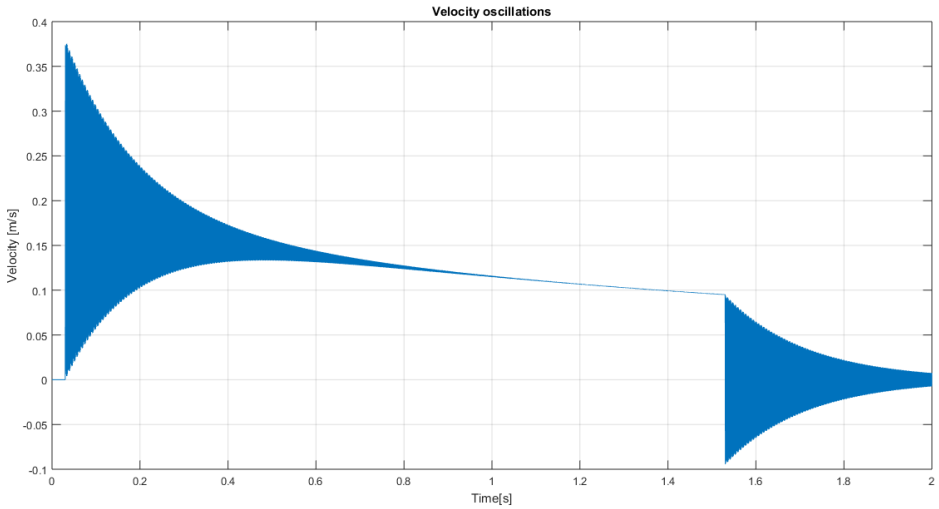

Figure 4-21 Velocity of the node 20 (Simulation of 20 nodes)

As it can be seen, the smaller the node, the wider the oscillations. The initial oscillations of the node 3 vary from 0 m/s to approximately 0.25 m/s while the oscillations of the node 20 go from 0 m/s to approximately 0.35 m/s. To see better the oscillations of the node 20, Figure 4.22 shows a zoom on the graph of the velocity of the node 20. Another conclusion is that the smaller the node, the more it takes to reach the steady state, and also the initial velocity of the node is higher.

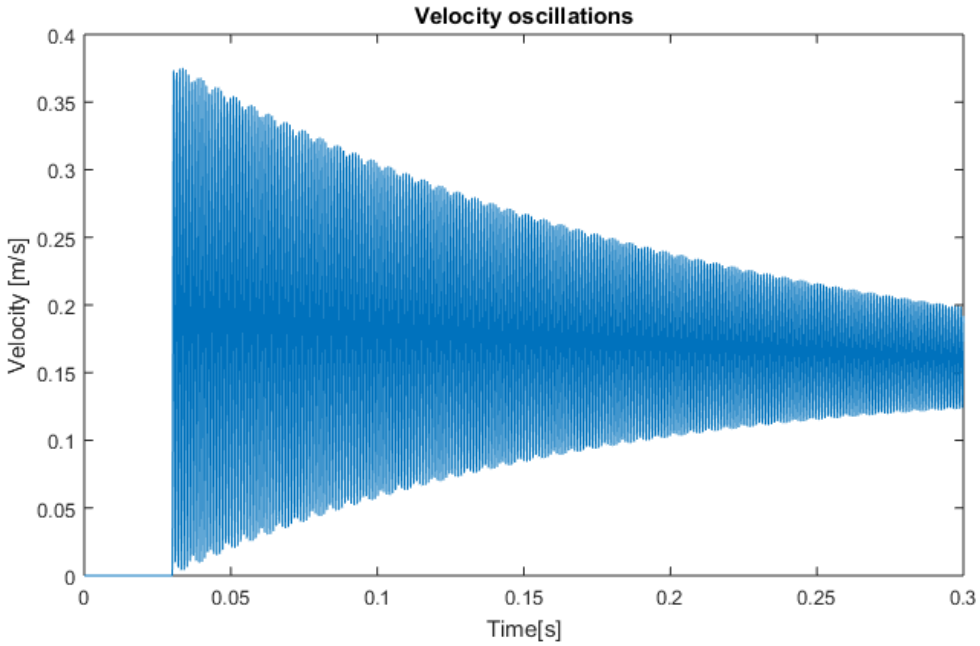

Figure 4-22 Zoom of the node 20's oscillations

Going back to the general view of the velocity graphics, it is visible that the internal nodes (the more distant to the entrance of pressure) have a softer variation of velocity while the more external nodes are the ones that have a wider variation of the speed.

Now is time to compare the graphs of the linearized system and the response of the model in front of a step signal. The difference between the Figures 4.3, 4.4, 4.5 and 4.6 is the time it takes the linearized system to reach the steady state: for the 3-node model is less than for the 20-node model. And that is visible in both Figure 4.10, 4.11, 4.18 and 4.19, where the oscillation time of the model is wider for the 20-node model than for the 3-node model.

4.6. Experimental results

4.6.1. Test Station 4

The Test Station 4 is placed in the laboratory of Fuel Cell Control of the "Institut de Robòtica i Informàtica Industrial" (Institute of Robotics and Industrial Informatics) of the UPC. This laboratory is used for the validation and testing of control strategies of fuel cell based energy conversion system. The Figure 4.23 shows the Test Station 4.

Figure 4-23 PEM water-cooled system of Test Station 4

Besides the PEM fuel cell itself, an ejector based on the venturi effect has been designed and implemented in the system (Figure 4.24).

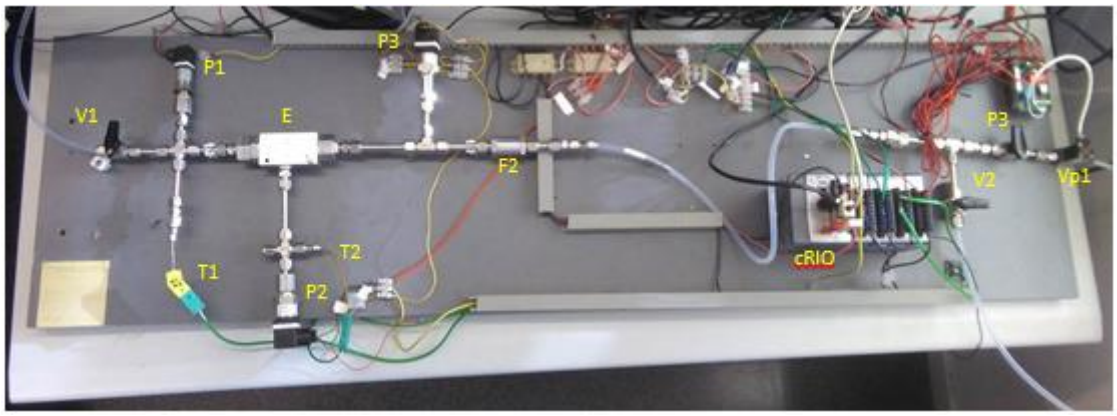

Figure 4-24 Venturi ejector system

The general layout of the feeding channel including the ejector is shown in Figure 4.25 and the different components are named in the Table 4.2.

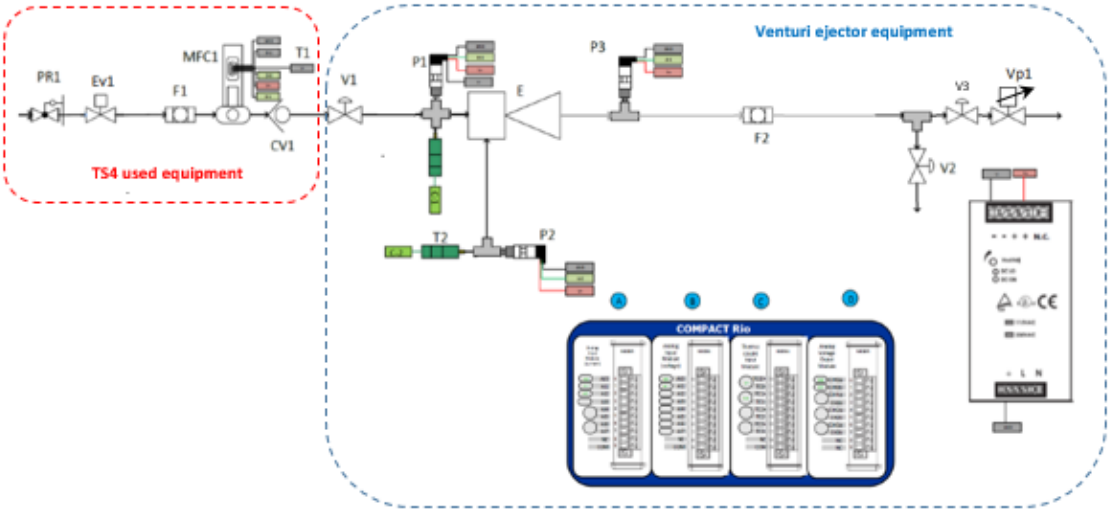

Figure 4-25 Equipment layout

Abbreviation	Name
PR1	Pressure regulator
Ev1	Solenoid valve
F1, F2	Particle filter
MFC1	Hydrogen mass flow meter
CV1	Non-return valve
V1, V2, V3	Ball valves
Vp1	Proportional control
cRIO	COMPACT RIO (real time data acquisition)
P1, P2, P3	Pressure transducers

Table 4-2 Abbreviations and names of the system components

4.6.2. Comparison

To reproduce a closed pipe, the ball valves V2 and V3 are closed and only the V1 is opened, letting the gas flow in. The pressure at the entrance of the channel will be compared with the measured pressure of P1 and the velocities will be compared to the gas flow measured with MFC1. The signal sampling is not as frequent as the one used in the simulation results. That means that the comparison will be qualitative and not quantitative.

The results of the experiment in the Test Station 4 are shown in the Figure 4.26.

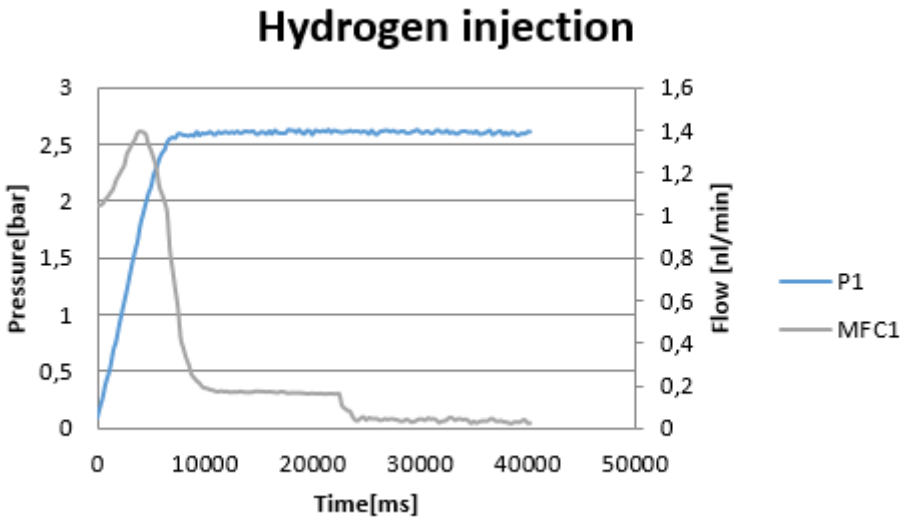

Figure 4-26 Experimental results of the filling of the channel

The graph shows a similar evolution of the system to the graphs obtained with the simulations. The pressure increases really quickly and when it reaches a certain value it keeps constant. Concerning the flow, it raises a little at the beginning of the process and it starts decreasing when the pressure gets constant. At the end the flow is 0 and constant.

5. MODELLING THE EXIT OF HYDROGEN

Now that the evolution of the system during the filling of hydrogen is known, it is time to go ahead and to modelize the exit of hydrogen. This exit flow is the one that will react in the PEM fuel cell.

5.1. Equations

The system is different from the one of the previous sections, meaning that some changes must be done on the equations. The study will focus only on the dynamics of the channel, that is why the main equations are the continuity equation and the Navier-Stokes equation.

5.1.1. Continuity equation

Now the system has a leak: the flow that will feed the fuel cell and generate the pertinent current.

The way to include this loss of mass in the equation (4.6) is adding a negative value-negative because the mass is leaving the system. The units of the loss must be in line with the units of the equation: kg/m^3.

$$\frac{\partial \rho}{\partial t} = -u\frac{\partial \rho}{\partial z} - \rho\frac{\partial u}{\partial z} - \frac{\dot{m}}{V} \tag{5.1}$$

Where:

- $\dot{m}$: mass flow of the hydrogen leak [kg/s]

5.1.2. Navier-Stokes equation

For this equation no changes have to be done. But there is a component that depends directly on the continuity equation, and there so, it will have to be replaced by the new equation (5.1).

The equation (4.9) now will result as the following one:

$$u\frac{\partial \rho}{\partial t} = u(-u\frac{\partial \rho}{\partial z} - \rho\frac{\partial u}{\partial z} - \frac{\dot{m}}{V}) = -u^2\frac{\partial \rho}{\partial z} - u\rho\frac{\partial u}{\partial z} - u\frac{\dot{m}}{V} \tag{5.2}$$

And if the term is replaced in the equation (4.17):

$$-u^2\frac{\partial\rho}{\partial z} - u\rho\frac{\partial u}{\partial z} - u\frac{\dot{m}}{V} + \rho\frac{\partial u}{\partial t} = -\frac{RT\partial\rho}{M\partial z} + \rho\nu\frac{\partial^2 u}{\partial z^2} + \frac{\partial\rho}{\partial z}\nu\frac{\partial u}{\partial z} \tag{5.3}$$

If now the term of the variation of velocity through time is isolated, the final equation will result:

$$\frac{\partial u}{\partial t} = \frac{u^2}{\rho}\frac{\partial\rho}{\partial z} + u\frac{\partial u}{\partial z} + \frac{u}{\rho}\frac{\dot{m}}{V} - \frac{RT\partial\rho}{\rho M\partial z} + \nu\frac{\partial^2 u}{\partial z^2} + \frac{\partial\rho}{\partial z}\frac{\nu}{\rho}\frac{\partial u}{\partial z} \tag{5.4}$$

5.2. Equilibrium points study

The ejection of hydrogen is applied only for a few seconds so the system can recovery the losses and then been applied again.

Once the leak has been applied, the equilibrium points are the same that the ones on the section 4.3. The system will reach the steady state when all the nodes have the same density and it is proportional to the external pressure, and when the velocities are zero.

There so, the expected evolution of the system after the ejection of hydrogen, is that the density increases from the final value to the same density that had before the leak.

5.3. Simulation

5.3.1. Preparations for the simulation

To avoid sudden changes that could lead to an error during the integration, the exit mass flow has been modelled as a combination of ramps, with a saturation period between them.

The leak value depends on the mass flow and on the volume of the node. The equation of the volume is [9]:

$$V = \pi r^2 z \tag{5.5}$$

Where:

- π : is the pi constant
- r : is the radius of the cylinder

The values of the parameters and the initial conditions are shown on the table 5.1.

Constants	Value	Units
n	5-10	-
z	$\frac{0.3}{n}$	m
$\dot{m}$	1.5e-8	$\frac{kg}{s}$
r	0.0005	m
π	3.14159265359	-

Table 5-1 Names, values and units of the parameters and initial conditions

In order to see better the behaviour of the system, the hydrogen leak will occur once the feeding of the channel has reached the steady-state. There so the simulations last 7 seconds, the leak starts at the second 3 and finishes at the second 6. The overall behaviour of the leak flow is shown in the figure 5.1.

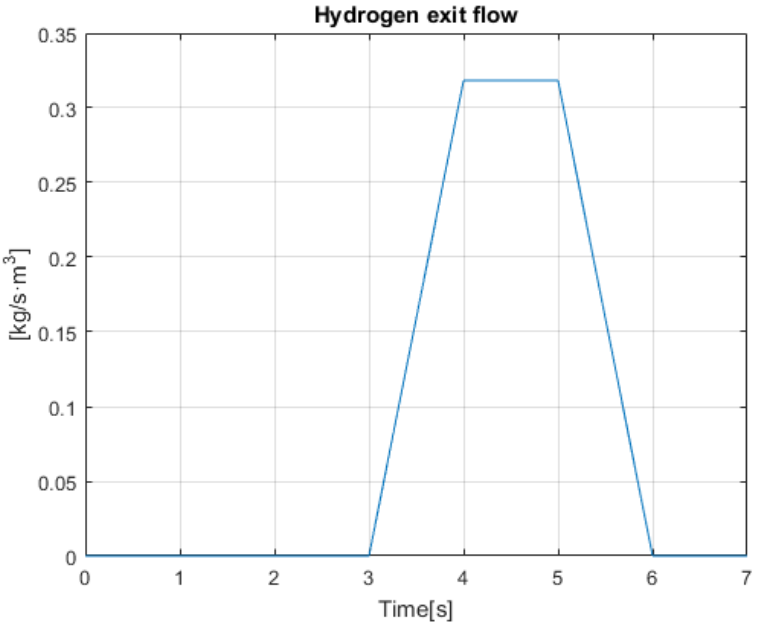

Figure 5-1 Hydrogen exit flow

5.3.2. Simulation with 5 nodes

The first simulation has been done on the model with 5 nodes applying the equations 5.1 and 5.4 on the node 3. The results of both the velocities and densities are shown in this section.

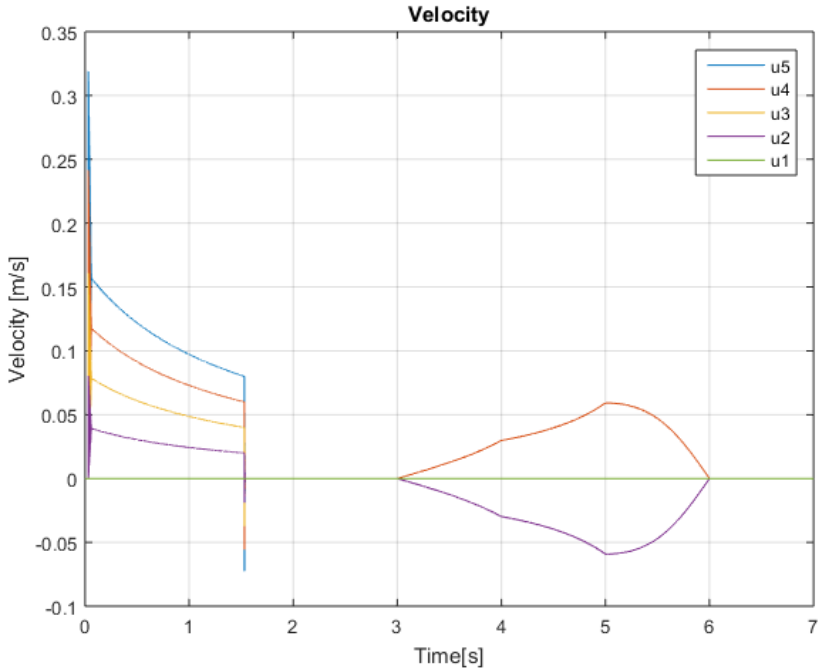

Figure 5-2 Velocities of the simulation with 5 nodes

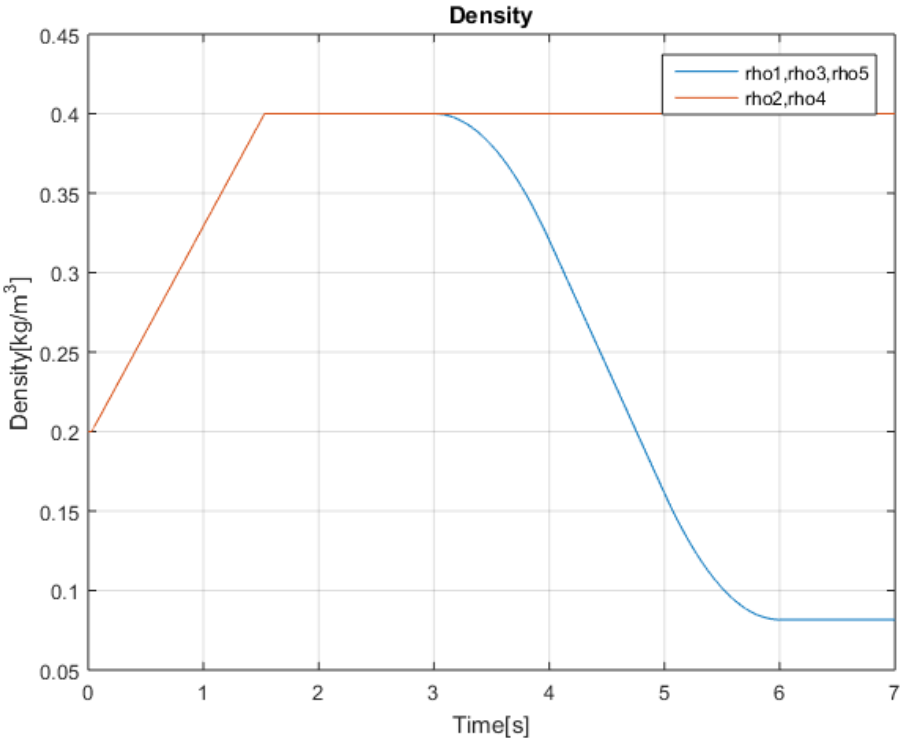

Figure 5-3 Densities of the simulation with 5 nodes

5.3.3. Simulation with 10 nodes

The second one has been done on the model with 10 nodes to observe better how the different nodes react in front of the mass flow. For this simulation the equations 5.1 and 5.4 had been applied on the node 6.

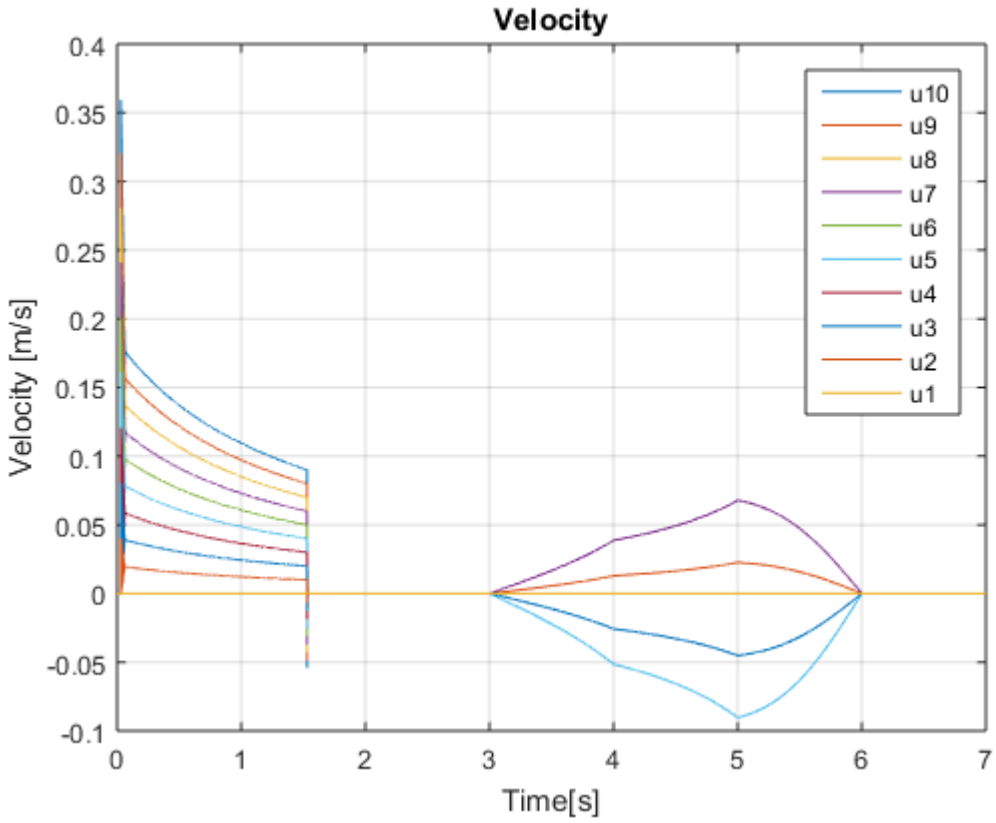

Figure 5-4 Velocities of the simulation with 10 nodes

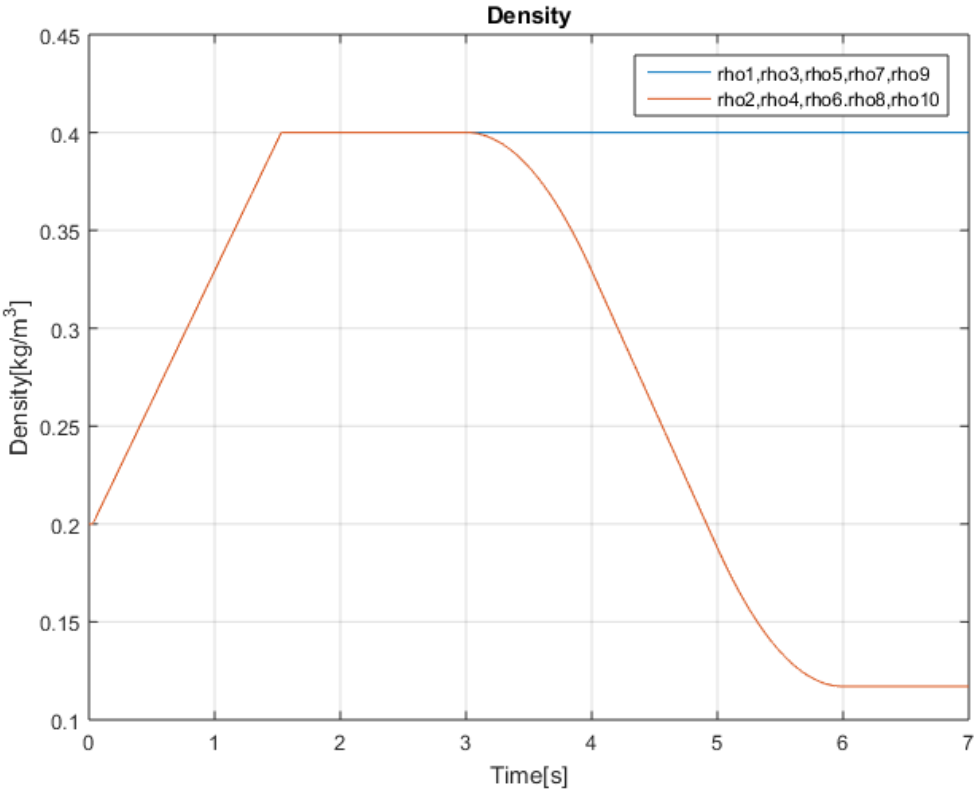

Figure 5-5 Densities of the simulation with 10 nodes

However, in the real case, the exit of hydrogen will not be punctual. In order to observe the behaviour of the system when the leak has been applied on the adjacent nodes. The evolution of the system modifies based on the combination of nodes with ejection of the gas. To keep constant the total mass being ejected, for the following simulations the value of $\dot{m}$ is 0.5 e-8 kg/s

If the leak is applied on the nodes 5, 6 and 7 all the velocities that appear are positive and some densities increase (Figures 5.6 and 5.7).

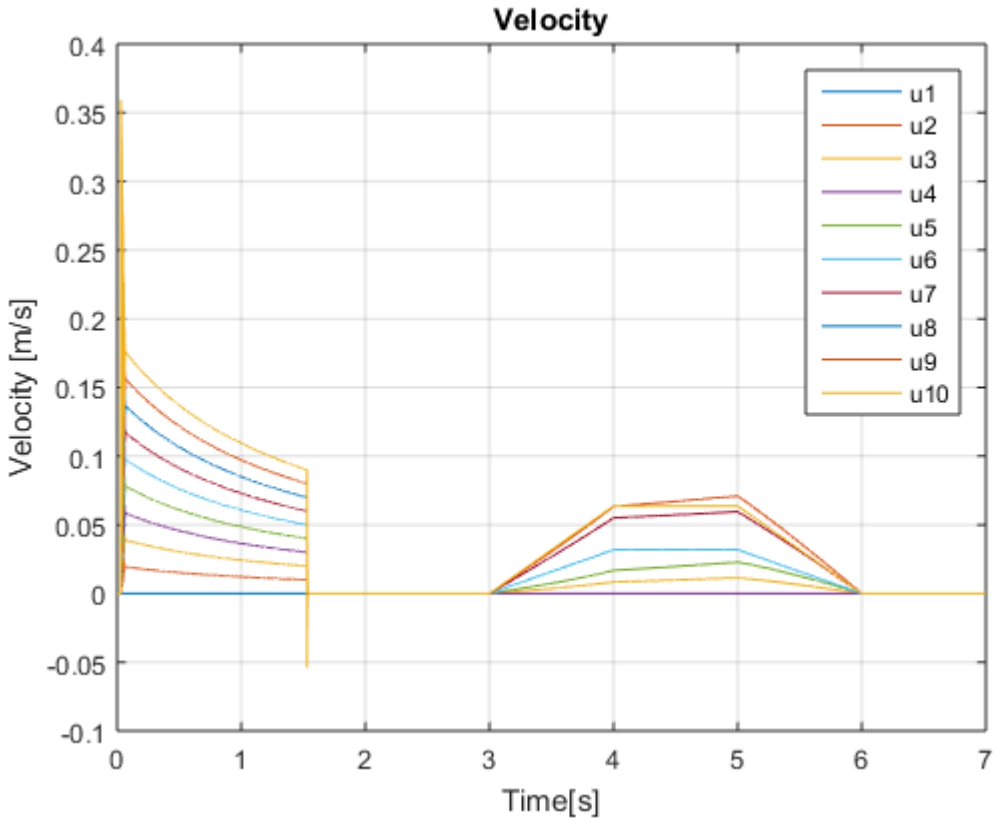

Figure 5-6 Velocities of the system with the leak applied on the nodes 7, 6 and 5

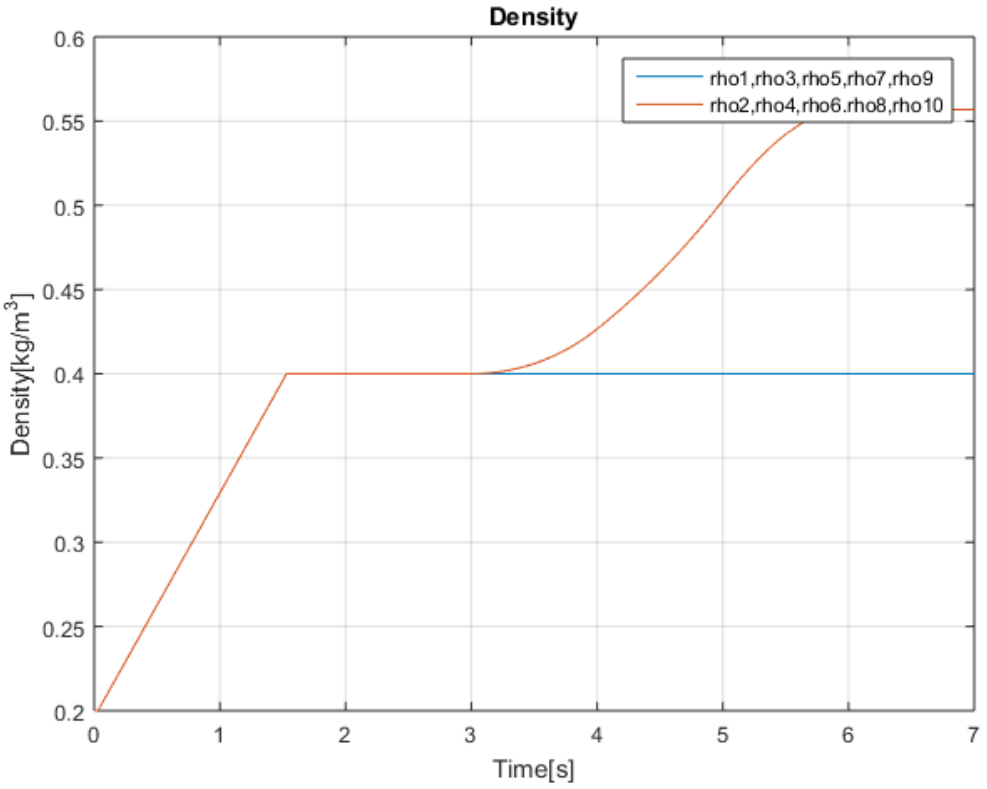

Figure 5-7 Densities of the system with the leak applied on the nodes 7, 6 and 5

If the combination of nodes is 6, 5 and 4, almost all the velocities are positive (Figure 5.8) and the densities decrease (5.9).

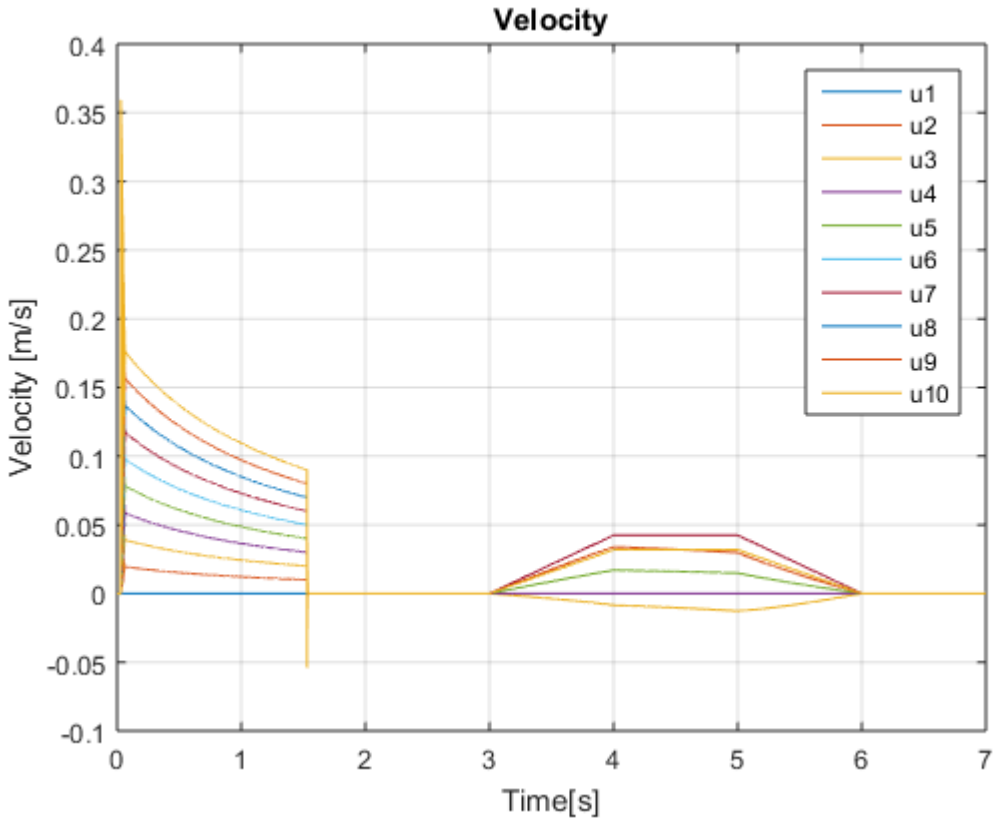

Figure 5-8 Velocities of the system with the leak applied on the nodes 6, 5 and 4

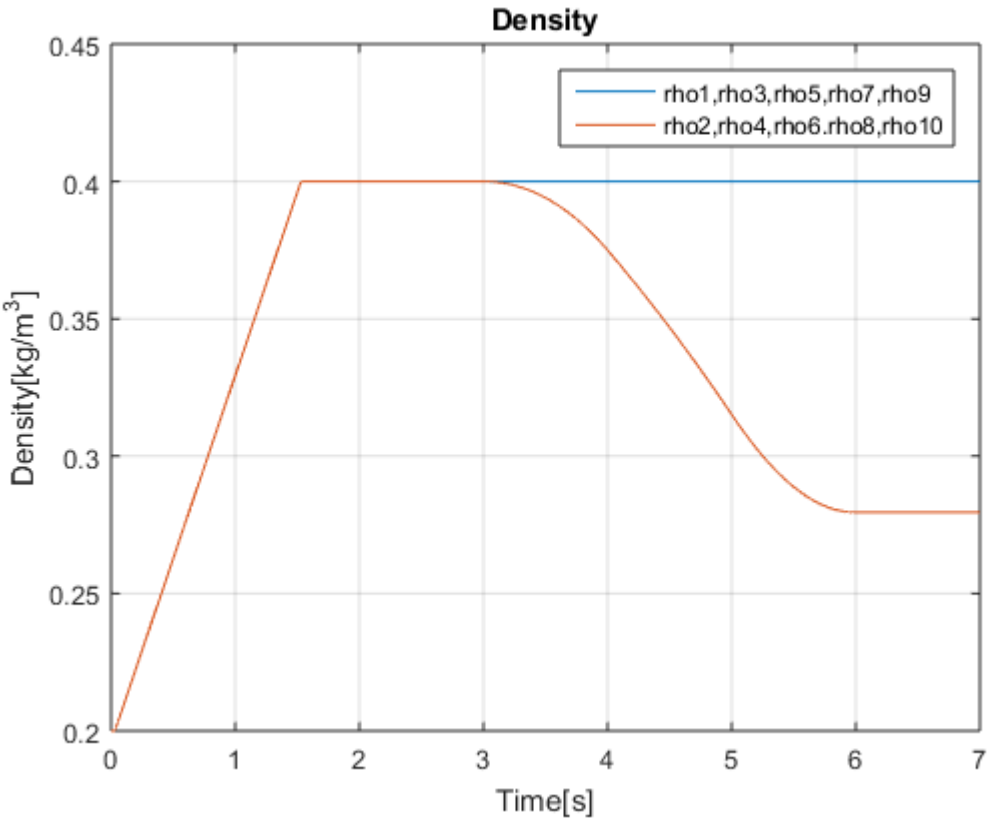

Figure 5-9 Densities of the system with the leak applied on the nodes 6, 5 and 4

The last sequence of nodes is nodes 8, 7 and 6. In this case the densities also decrease and the velocities are positive and negative (Figures 5.10 and 5.11).

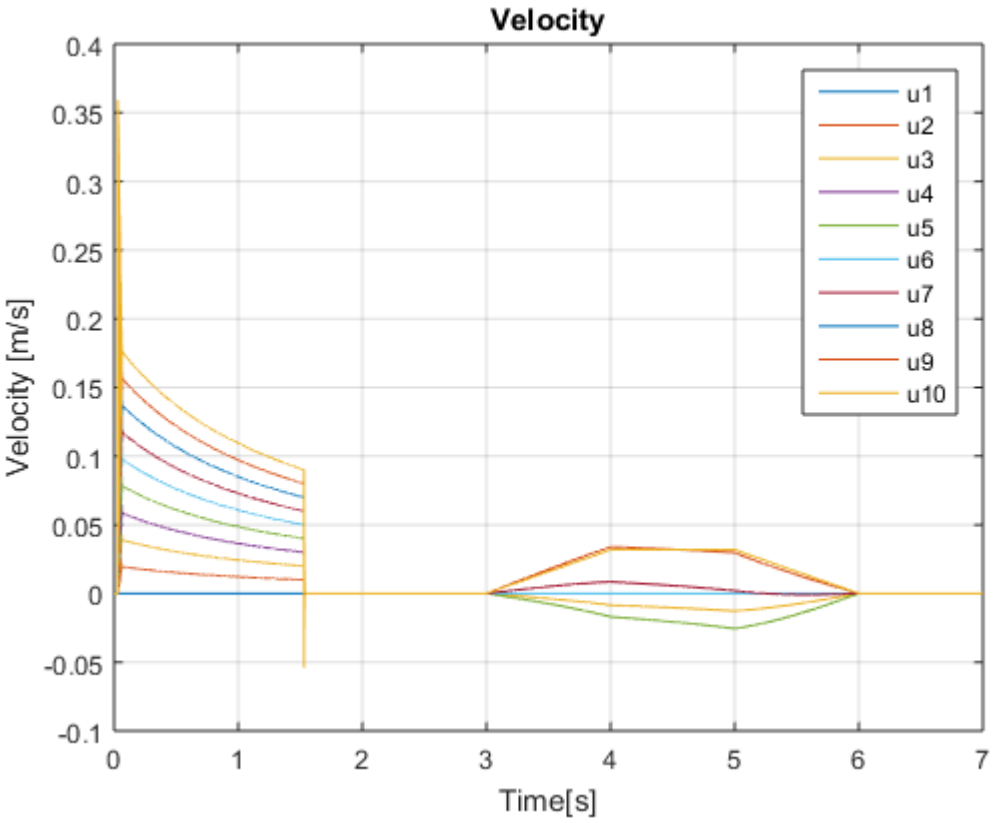

Figure 5-10 Velocities of the system with the leak applied on the nodes 8, 7 and 6

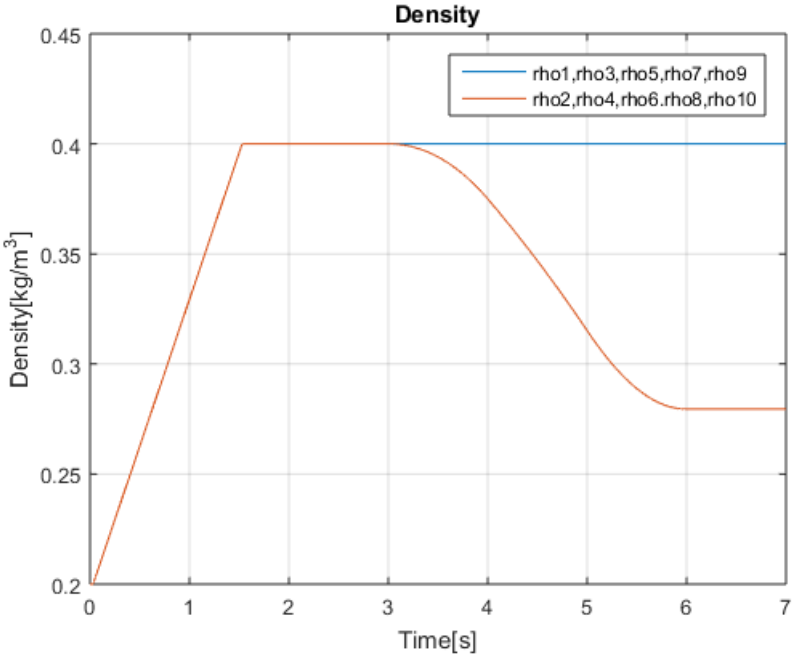

Figure 5-11 Densities of the system with the leak applied on the nodes 8, 7 and 6

5.3.4. Comparison of the results

Once the simulations had been done, is time to compare and analyze the results in order to reach conclusions.

If the study is focused on the densities, both graphs are quite similar (Figures 5.3 and 5.5). The main difference is the final value of the density. The density depends on the mass flow and on the volume of the node (5.1), and the volume depends on the length of the node, which is different depending on the number of nodes. In both simulations, the node that suffers the loss of gas decreases its density, but the adjacent nodes maintain the density constant. This is not possible, the system should reach a steady-state where all the nodes have the same density. The mistake might be in the discretization of the equations: the node next to the most external node always has a density proportional to the external pressure.

Concerning the velocities, it seems that the loss of gas in a particular node changes the velocities in the rest of the system but not in the node itself. The reason why there are negative velocities is that the gas flows back due to the leak. As well, the positive velocities are due to the gas flowing forward. In the case of the 5-node the leak is applied on the node 3, the central node, and that is the reason why the velocities are symmetric. In the Figure 5.4, the velocities are not symmetric, the reason is that the leak is not applied on the central node. As it can be seen on the Figure 5.4, there are different velocities and a statement can be done: the closer the node to the leak the higher the velocity.

The results of the different combinations of nodes with ejection of hydrogen require a deeper study in order to get proper conclusions. The Figure 5.7 shows how the density of the node 6 increases even though its density equation includes an exit of mass. Figures 5.9 and 5.11 show a similar graph to 5.5. The only difference is the final value of the density, as it has been said, the mass flow has been reduced to a third part.

The results of the velocities are a little bit more complicated to understand. The Figure 5.6 shows that all the velocities are positive, which means that all the internal flows go forward. If there are some nodes increasing their density, others should lose mass, meaning that the flow should go backwards. Another feature is that the velocities of the nodes 10 and 6 are constant during the seconds 4 and 5, while the rest of densities increase a little.

In the Figure 5.8 appears a negative velocity that belongs to the node 3, which means that the mass is flowing backwards. The velocities of the nodes, 10, 8 and 7 are the same, and as the node 6, they remain constant for one second. In this situation, the rest of velocities either decrease or are zero. For the last combination (nodes 8,7 and 6), there are both positive and negative velocities.

6. BUDGET

For the development of this project, the budget can be divided in the staff budget and the equipment budget.

For the staff budget it has been kept in mind the laboratory technician and the person responsible of the project itself. The salary is different for each one due to the experience and knowledge (Table 6.1).

Staff position	Salary (euro/hour)
Student	6
Laboratory technician	20

Table 6-1 Staff Salary

The overall staff budget is shown in Table 6.2. The working hours have been classified depending on the purpose of the work.

Staff position	Work purpose	Number of hours	Cost (euro)
Student	Research	20	120
	System modelling	120	720
	Simulations and analysis	90	540
	Project Composition	50	300
Laboratory technician	Data acquisition	1	20
TOTAL			1700

Table 6-2 Staff Budget

Besides the personnel costs, the equipment budget (Table 6.3) has been calculated.

Object	Units	Price (euro)	Service life (months)	Consumption (months)	Cost (euro)
Laptop	1	700	60	5	58.33
MatLab Student License	1				35
TOTAL					93.33

Table 6-3 Equipment budget

The costs of the Test Station 4, the hydrogen used for the experiments and the electricity used for the data acquisition is not reflected on the budget. The reason is that the experimental data is from older experiments and the costs have not been saved.

The total budget of the project can be seen on Table 6.4.

Budget	Cost (euro)
Staff budget	1700
Equipment budget	93.33
TOTAL	1793.33

Table 6-4 Project budget

7. ENVIRONMENTAL IMPACT

The nature of this project is purely theoretical, there so the impact on the environment is quite low. Just the energy that has been used to run the laptop during the simulations period and during the composition of the project. The origin of the used energy is unknown, so that is why is impossible to affirm that the energy comes from renewable resources. There so, the impact of the energy consumption cannot be submitted.

However, the purpose of this project is to improve the operation of a PEM fuel cell and make it more efficient. The actual energy resources, based on the combustion of solid fuels, could be easily replaced by the PEM fuel cells. It is true that a lot of work must be done in order to improve them, but the environmental advantages are quite notorious. The PEM fuel cells are silent due to the lack of moving parts in their system. They work with hydrogen so the emissions are really low and the products are water and heat. Compared to high CO_{2} emissions of the solid fuels, the use of PEM fuel cells is much more eco-friendly. Also, the lifetime of this source of energy is much longer than the solid fuels.

The implementation of the PEM fuel cells on the machines used on a daily basis would reduce the emissions and improve the quality of the environment.

8. CONCLUSIONS

The purpose of this project is to design a valid model for the filling of the feeding channel in a PEM fuel cell and also the ejection of the reactant gas. If the model is correct, the following stages of the recirculation should be applied on it, such as the entrance of water in the pipe, nitrogen. Then the recirculation of the non-reactant hydrogen, and last but not least, the control of the water purges.

After the analysis of the simulations' results, the model does not reflect a correct operation for the ejection of gas. The reason is the discretization that has been done on the continuity and Navier-Stokes equations.

There so, this section of the project should be looked over and modified. Then the simulations must be repeated to affirm that the new model works properly and then move on to the next stages.

9. BIBLIOGRAPHY

[1] Barbir, Frano, 2005. *PEM Fuel Cells: Theory and Practice*. Elsevier Academic Press

[2] Andújar, J.M., Segura, F., 2009. *Fuel cells: History and updating. A walk along two centuries*.Elsevier

[3] Siegel, J., McKay, D., Stefanopoulou, A., Hussey, D., and Jacobson, D., 2008. *Measurement of liquid water accumulation in a PEMFC with dead-ended anode*. Journal of Electrochemical Society, 155, pp. B1168–B1178.

[4] Chen, J., Siegel, J., Stefanopoulou, A., 2012 *Optimization of purge cycle for dead-ended anode fuel cell operation*.ASME

[5] Pedlosky, J., 1982 *Geophysical Fluid Dynamics* Springer p. 10-11

[6] Kaplan, W., 5th edition *Advanced Calculus.* Pearson p. 181

[7] Acheson, D. J., 1990 *Elementary Fluid Dynamics.* Oxford University Press. p. 205

[8] Kaufman, M., 2002. *Principles of Thermodynamics.* Marcel Dekker p. 6

[9] Swokowski, E. W., 1979 *Calculus with Analytic Geometry* Prindle, Weber & Schmidt Marcel Dekker p. 6A33